RECLAMATION

Managing Water in the West

Technical Report No. SRH-2015-33

2D and 3D Flow Modeling along Fremont Weir Section of the Sacramento River in Support of Fish Tracking

U.S. Department of the Interior
Bureau of Reclamation

January 2016

Mission Statements

The mission of the Department of the Interior is to protect and provide access to our Nation's natural and cultural heritage and honor our trust responsibilities to Indian Tribes and our commitments to island communities.

The mission of the Bureau of Reclamation is to manage, develop, and protect water and related resources in an environmentally and economically sound manner in the interest of the American public.

Cover Photo: Sacramento River north of Fremont Weir (photo from survey crew)

Technical Report No. SRH-2015-33

2D and 3D Flow Modeling along Fremont Weir Section of the Sacramento River in Support of Fish Tracking

Prepared by

_____ _____

Yong G. Lai, Ph.D., Hydraulic Engineer **Date**
Sedimentation and River Hydraulics Group
Technical Service Center
Denver, Colorado

Peer Reviewed by:

_____ _____

Josh Israel, Fish Biologist **Date**
Bay-Delta Office, Mid-pacific Region
Sacramento, California

U.S. Department of the Interior
Bureau of Reclamation

January, 2016

Table of Contents

Page

1. Background 4
2. Numerical Models 7
   2.1 SRH-2D 7
   2.2 U^2RANS 8
3. Description of Study Site and Available Data 10
   3.1 Model Domain 10
   3.2 Field Data 12
4. Numerical Model Development 16
   4.1 Low Resolution Model 16
   4.1.1 Mesh and Terrain 16
      4.1.2 Roughness Representation 19
      4.1.3 Boundary Conditions 22
   4.2 High Resolution Model 26
      4.2.1 Mesh and Terrain 27
      4.2.2 Boundary Conditions 31
5. Low Resolution 2D Model Results 33
   5.1 Calibration Study 33
   5.2 Verification Study 46
   5.3 High Resolution Results 50
6. High Resolution 3D Model Results 51
   6.1 2D Simulation Results 51
   6.2 3D Model Results 53
      6.2.1 Low Discharge Results 54
      6.2.2 High Discharge Results 66
7. References 77

Index of Figures

Page

Figure 1. Study area near Fremont Weir, Sacramento River, California 5
Figure 2. Low resolution model domain developed for the modeling of the Sacramento River (Dynamic Solutions, 2011) 11
Figure 3. High resolution model domain used for U2RANS modeling of the Sacramento River near Fremont Weir, the Sacramento River, California..... 12
Figure 4. 2015 bathymetric survey spatial extent and data points 14
Figure 5. Bed elevation contours in the big bend area of the High-Res-3D model based on the 2015 survey data 14
Figure 6. Bed elevation contours in the big bend area of the High-Res-3D model based on the 1997-2000 ADH high resolution model..... 15
Figure 7. 2D mesh of the low resolution model domain: Overview 17
Figure 8. Close-up views of the 2D mesh for the Low-Res-2D model domain in the Fremont Weir area 18
Figure 9. Eighteen zones of the Manning's roughness coefficient for the Low-Res-2D model: entire model domain 20
Figure 10. Zones of the Manning's roughness coefficient in Freemont Weir area..... 21
Figure 11. Flow hydrographs at seven inflow boundaries of the Low-Res-2D model from December 12, 2010 to March 1, 2011..... 24
Figure 12. Stage recorded at the Freeport for the Low-Res-2D model from December 12, 2010 to March 1, 2011 24
Figure 13. Flow hydrographs at seven inflow boundaries of the Low-Res-2D model from December 1, 2014 to March 31, 2015..... 25
Figure 14. Stage recorded at Freeport for the Low-Res-2D model from December 1, 2014 to march 31, 2015 25
Figure 15. An overview of the 2D mesh developed for the High-Res-3D model..... 27
Figure 16. A close-up view of the High-Res-3D mesh at the big bend area of the Fremont Weir section 28
Figure 17. A close-up view of the High-Res-3D mesh at the confluence of the Sacramento River and the Feather River 28
Figure 18. 2015 terrain represented by the High-Res-3D mesh: entire domain view..... 29
Figure 19. 2015 terrain represented by the High-Res-3D mesh: the upstream section at the big bend area (1:5 vertical distortion)..... 30
Figure 20. 2015 terrain represented by the High-Res-3D mesh: the downstream section of the big bend area (1:5 vertical distortion) 30
Figure 21. Flow discharges at the Knights Landing and Feather River for the period of December 1, 2014 to march 31, 2015 32
Figure 22. Stage at Verona gauge for the period of December 1, 2014 to March 31, 2015 32

Figure 23. Gauge locations for Low-Res-2D model calibration (Dynamics Solutions, 20110) 34
Figure 24. Comparison of simulated and recorded stage at I-Street Bridge gauge between December 12, 2010 and March 1, 2011 36
Figure 25. Comparison of simulated and recorded stage at Verona gauge between December 12, 2010 and March 1, 2011 36
Figure 26. Comparison of simulated and recorded stage at Fremont Weir gauge between December 12, 2010 and March 1, 2011 37
Figure 27. Comparison of simulated and recorded stage at Knight's Landing gauge between December 12, 2010 and March 1, 2011 37
Figure 28. Comparison of simulated and recorded discharge at Freeport gauge between December 12, 2010 and March 1, 2011 38
Figure 29. Comparison of simulated and recorded discharge at Verona gauge between December 12, 2010 and March 1, 2011 39
Figure 30. ADCP transect locations within the study area with white colored dots representing transects (Hammack et al, 2013a) 40
Figure 31. Depth-averaged velocity comparison on Transects 1 to 4 between Low-Res-2D and ADCP data 41
Figure 32 Depth-averaged velocity comparison on Transects 5 to 10 between Low-Res-2D and ADCP data 41
Figure 33. Depth-averaged velocity comparison on Transects 11 to 14 between Low-Res-2D and ADCP data 42
Figure 34. Depth-averaged velocity comparison on Transects 15 to 19 between Low-Res-2D and ADCP data 42
Figure 35. Depth-averaged velocity comparison on Transects 20 to 24 between Low-Res-2D and ADCP data 43
Figure 36. Depth-averaged velocity comparison on Transects 25 to 27 between Low-Res-2D and ADCP data 43
Figure 37. Depth-averaged velocity comparison on Transects 28 to 32 between Low-Res-2D and ADCP data 44
Figure 38. Depth-averaged velocity comparison on Transects 33 to 36 between Low-Res-2D and ADCP data 44
Figure 39 Depth-averaged velocity comparison on Transects 37 to 39 between Low-Res-2D and ADCP data 45
Figure 40. Depth-averaged velocity comparison on Transects 40 to 42 between Low-Res-2D and ADCP data 45
Figure 41. Comparison of simulated and recorded stage at I-Street Bridge gauge between December 1, 2014 and march 31, 2015 47
Figure 42. Comparison of simulated and recorded stage at Verona gauge between December 1, 2014 and March 31, 2015 47
Figure 43. Comparison of simulated and recorded stage at Fremont Weir gauge between December 1, 2014 and March 31, 2015 48

Figure 44. Comparison of simulated and recorded stage at Knight's Landing gauge between December 1, 2014 and March 31, 2015 48
Figure 45. Comparison of simulated and recorded discharge at Freeport gauge between December 1, 2014 and March 31, 2015 49
Figure 46. Comparison of simulated and recorded discharge at Verona gauge between December 1, 2014 and March 31, 2015 49
Figure 47. Comparison of High-Res-2D2 simulated and gauge discharges at Verona between December 1, 2014 and April 1, 2015 52
Figure 48. Comparison of High-Res-2D2 simulated and gauge stage at the Fremont Weir between December 1, 2014 and April 1, 2015 53
Figure 49. Ten (10) transects where the ADCP measurement was carried out in January-February, 2015 54
Figure 50. Comparison of depth-averaged velocity along 10 transects between 3D, 2D and ADCP results for the Low-Q run on January 26, 2015 59
Figure 51. High-Res-3D predicted (top) and ADCP measured (bottom) secondary flow patterns at 10 transects for the Low-Q run 66
Figure 52. Comparison of depth-averaged velocity along 10 transects between 3D, 2D and ADCP results for the High-Q run on February 11, 2015 71
Figure 53. High-Res-3D predicted (top) and ADCP measured (bottom) secondary flow patterns at 10 transects for the High-Q run 76

Index of Tables

Page

Table 1. Manning's coefficients used by Low-Res-2D model within 18 zones 21
Table 2. Stations used to develop the boundary conditions (Source: Dynamic Solutions, 2011) 26
Table 3. Sacramento River gauges used for model calibration..... 34

Summary

Both two-dimensional (2D) and three-dimensional (3D) numerical modeling are carried out for flow hydraulics along the Fremont Weir section of the Sacramento River, California. Numerical results are generated to support the Eulerian-Langrangian Agent Method (ELAM) modeling of fish movement to be carried out by engineers at the U.S. Corps of Engineers (USACE). The model results can also be used to understand fish migration behaviors and statistical patterns in relation to local flow dynamics when coupled with the telemetry fish tracking data. The flow results and ELAM modeling may also be used to assist the Fremont Weir notch design to achieve the desired fish migration through the Yolo Bypass. This work is part of a larger effort related to the Yolo Bypass EIS/EIR study for fish survival. Participants include Reclamation Bay Delta Office, Department of Water Resources (DWR) of California, USACE Engineering Research & Development Center (ERDC), and USACE Sacramento District.

The SRH-2D low-resolution model covers about 69 miles of the Sacramento River. It starts at the Freeport (river mile 47.6) downstream and ends at Wilkins Slough (river mile 117) upstream. Also, the model includes part of the Feather River and American River. The 2D low-resolution model is based on the same mesh developed by Dynamic Solutions LLC (2011) and Hammack et al. (2013a) who used ADH for 2D modeling. So the present SRH-2D model can not only be calibrated and verified with the available gauge and ADCP data, it can also be compared with ADH model results. The SRH-2D low-resolution model serves the following two purposes: (a) it provides the missing boundary conditions to the high-resolution model since all boundaries of the low-resolution model are located near flow gauge stations; and (b) it offers another 2D model for the project that is calibrated and verified. Two simulations are carried out: One for December 2010 – March 2011 period and another for December 2014 – March 2105 period. Comparisons of the 2D low-resolution model with the available gauge data lead to the following conclusion:

- The SRH-2D low-resolution model agrees with the ADH model results very well. SRH2D and ADH used quite different numerical methods, discretization schemes, and physical process models such as turbulence and energy loss equations. Close agreement between the two proves that both models have solved the same set of governing equations correctly.
- The model results agree with the recorded stage and discharge at several gauge stations over most of the period. The exception is that the stage and discharge are under-predicted at high flows. The under-prediction may be attributed to unaccounted inflows and outflows through the model domain.

- The SRH-2D low-resolution model results compare well with the ADCP velocity data on 42 measured transects. This provides further credence to the numerical model in its ability to predict the flow velocity through the river system.

2D model, however, does not provide vertical velocity information. Secondary flow patterns are deemed important for fish migration and are not predicted by 2D models. It calls for 3D modeling of the study area.

The 3D U^2RANS high-resolution model is developed in this study, based on the 2015 bathymetric data, in order to predict secondary flows and other 3D flow patterns. The 3D model encompasses about 18-km reach along the Fremont Weir section. The model domain has an increasingly refined mesh and is only a subdomain of the 2D low-resolution model. The high-resolution model starts from Knight Landing upstream and ends at Verona gauge downstream. Both SRH-2D and 3D U^2RANS simulations are formed with the high-resolution model. SRH-2D results for the December, 2014 – March 2015 time period are compared with the gauge discharge and stage data with good agreement. Further, both 2D and 3D fine-resolution models are compared with the ADCP measurements at ten transects at two dates.

Comparison of the 2D and 3D fine-resolution model results with the 2015 ADCP data leads to the following findings:

- Both 2D and 3D models predict very well the depth-averaged velocity as measured by the ADCP.
- 2D and 3D depth-averaged velocities are very similar to each other confirming that 2D models are adequate in predicting depth-averaged velocities in natural rivers with even sharp bends.
- The main advantage of 3D models is the ability to predict secondary flow patterns and local velocity impacted by in-stream structures. A comparison of the 3D predicted secondary flows with the ADCP observed data shows that the 3D captures the secondary flow patterns observed at most of the ten transects of the ADCP data. High discrepancy is observed only at transect 8 at low flow near the end of the big bend. This mismatch at transect 8 may be attributed to the inaccuracy in local bathymetry used by the model. Field study near transect 8 showed that the flow in the area was unsteady and subject to dynamic changes in bathymetry.

We may conclude by this study that the 3D fine resolution model is reliable in its ability to predict both the depth-averaged velocity and secondary flows along the

Fremont Weir section of the Sacramento River. The model now is ready to be applied to assist the weir notch design in FY 2016.

1.Background

This work is part of a larger effort related to the Yolo Bypass EIS/EIR study for fish survival. Participants include U.S. Bureau of Reclamation (Reclamation) Bay Delta Office, Department of Water Resources (DWR) of California, U.S. Geological Survey (USGS), US Army Corps of Engineers (USACE) Engineering Research & Development Center (ERDC), and USACE Sacramento District.

Two-dimensional (2D) and three-dimensional (3D) computational fluid dynamics (CFD) simulation is carried out to predict flow hydrodynamics along the Fremont Weir section of the Sacramento River, California. Flow hydrodynamic variables have a significant impact on fish movement behaviors. Therefore, CFD model results are generated by this study to support the Eulerian-Lagrangian Agent Method (ELAM) modeling of fish movement at the study site. The fish movement modeling portion of the study is to be carried out by engineers at the USACE. ELAM model takes hydrodynamic flow and turbulence data, coupled with bioenergetic data for specific species, to make probabilistic estimates of fish movement in an aquatic environment. In addition, CFD results may also be used in conjunction with the telemetry fish tracking data in the field to discern the fish behaviors and statistical patterns in relation to flow characteristics. Further, CFD model results may also play an important role in Fremont Weir notch design in that the desired flow characteristics beneficial to fish migration may be obtained.

The study site is the section of the Sacramento River along the Fremont Weir as shown in Figure 1. The primary interested area of the study covers about 10 km (about 6 miles) section of the Sacramento River with the downstream cross section located at the Verona station.

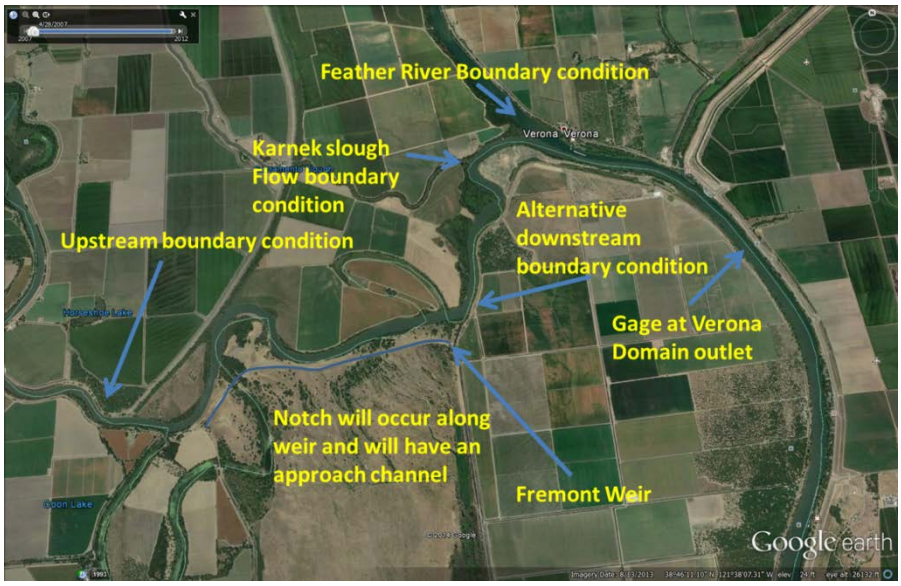

Figure 1. Study area near Fremont Weir, Sacramento River, California

The work scope consists of the following: (1) Data preparation and processing for numerical model use; (2) Numerical model development (both 2D and 3D models); (3) Model calibration; (4) Model verification and application; and (5) Final reporting.

A 2D hydraulic model is developed covering a long reach of the Sacramento River: about 115 km (69 miles) from Wilkins Slough upstream to Freeport downstream. We use the depth-averaged 2D model, SRH-2D, developed at the Bureau of Reclamation (Dr. Lai is the lead developer of SRH-2D). SRH-2D is a well-documented, successfully-verified, and widely-used 2D hydraulic model; and it has been adopted by several agencies. The 2D model models have the benefit of covering a much larger river reach than the 3D so that the flow domain can have its boundaries located at or near flow gauges. This way, boundary conditions are readily available from the recorded data. In this study, 2D results are also used to provide the missing boundary conditions for the 3D model simulation.

A 3D simulation is carried out using U^2RANS, a 3D Reynolds Averaged Navier-Stokes (RANS) solver. U^2RANS is a non-hydrostatic 3D CFD model developed by Dr. Yong Lai, the principal investigator of this study, when he was employed at the University of Iowa. The model has been tested and validated by numerous flow cases; it has also been applied to an extensive list of hydraulic engineering projects with great success. However, 3D CFD modeling is computationally intensive. The model domain is often limited to a small river section of several

miles. In this study, the 3D model domain is selected to be larger than the interested area in Figure 1. Its upstream boundary is located near the Knights Landing while the downstream is at the Verona gauge station. The 3D model domain is approximately 18 km (10.8 miles) longitudinally along the Sacramento River and includes the flows from the Feather River and the Karnek Slough.

Field data between December 2010 and March 2011 are available for carrying out the 2D modeling; they are used to calibrate the SRH-2D model. The flow hydrograph of this period covers both high flows and low flows, so it is ideal for model calibration. The highest flows just topped the Fremont Weir. The data set of this time period offers the following benefits in modeling: (a) coinciding with the available bathymetric data; (b) coinciding with the available ADCP data (one day); (c) coinciding with the fish track data; and (d) having the LIDAR for the levees that can be merged with the bathymetry to produce a continuous surface.

New field data have been collected between December 2014 and March 2015 by the survey team from USACE Sacramento District, ERDC, DWR, and USGS. The survey area is most limited to the area near the Fremont Weir shown in Figure 1. The survey team has deployed a fish tracking array at the Fremont Weir area in January-February, 2015. They have also obtained the bathymetric and ADCP data in the same area. The 2015 data set provides a good data set to verified the 2D model and validated the 3D model.

2. Numerical Models

2.1 SRH-2D

SRH-2D, Sedimentation and River Hydraulics - Two-Dimension, is used in this study for the large-domain modeling. SRH-2D is a 2D depth-averaged hydraulic and sediment transport model for river systems, developed at the Technical Service Center, Bureau of Reclamation. The hydraulic flow modeling theory and the User's Manual are available in the reports by Lai (2008; 2010). SRH-2D has been used extensively by U.S. governing agencies, universities and private consulting companies. It has been adopted as the agency model by Reclamation, Federal Highway Administration, and Taiwan Water Resource Agencies.

SRH-2D adopts the arbitrarily shaped cell method of Lai et al. (2003a, b), the finite-volume discretization method, and an implicit time integration scheme. The numerical procedure is very robust that SRH-2D can simulate simultaneously all flow regimes (sub-, super-, and trans-critical flows) and both steady and unsteady flows. A special wetting-drying algorithm makes the model very stable in handling flows over dry surfaces. The mobile-bed sediment transport theory has been documented by Greimann et al. (2008), Lai and Greimann (2010), and Lai et al. (2011). The mobile-bed module predicts vertical stream bed changes by tracking multi-size, non-equilibrium sediment transport for suspended, mixed, and bed loads, and for cohesive and non-cohesive sediments, and on granular, erodible rock, or non-erodible beds. The effects of gravity and secondary flows on the sediment transport are accounted for by displacing the direction of the sediment transport vector from that of the local depth-averaged flow vector.

Major capabilities of SRH-2D are listed below:

- 2D depth-averaged solution of the St. Venant equations (dynamic wave equations) for flow hydraulics;
- An implicit solution scheme for solution robustness and efficiency;
- Hybrid mesh methodology which uses arbitrary mesh cell shapes. In most applications, a combination of quadrilateral and triangular meshes works the best;
- Steady or unsteady flows;
- All flow regimes simulated simultaneously: subcritical, supercritical, or transcritical flows;
- Mobile bed modeling of alluvial rivers with a steady, quasi-unsteady, or unsteady hydrograph;

- Non-cohesive or cohesive sediment transport;
- Non-equilibrium sediment transport;
- Multi-size sediment transport with bed sorting and armoring;
- A single sediment transport governing equation for both bed load, suspended load, and mixed load;
- Effects of gravity and secondary flows at curved bends; and
- Granular bed, erodible rock bed, or non-erodible bed.

SRH-2D is a 2D model, and it is particularly useful for problems where 2D effects are important. Examples include flows with in-stream structures such as weirs, diversion dams, release gates, coffer dams, etc.; bends and point bars; perched rivers; and multi-channel systems. 2D models may also be needed if certain hydraulic characteristics are important such as flow recirculation and eddy patterns; lateral variations; flow overtopping banks and levees; differential flow shears on river banks; and interaction between the main channel, vegetated areas and floodplains. Some of the scenarios listed above may be modeled in 1D, but additional empirical models and input parameters are needed and extra calibration must be carried out with unknown accuracy.

2.2 U^2RANS

U^2RANS, Unsteady and Unstructured Reynolds Averaged Navier-Stokes, is a comprehensive general-purpose 3D CFD model. The model is highly accurate, well verified and validated, and widely used for many research and engineering projects. The model was developed more than a decade ago, while the report author was employed as a senior research staff and adjunct associate professor at the Iowa Institute of Hydraulic Research, the University of Iowa.

In the area of hydraulic engineering, successful applications of U^2RANS include:

- Flow hydrodynamics in rivers and lakes upstream of hydropower dams;
- Detailed flow characteristics around hydraulic structures;
- Hydraulic impact of project alternatives on fish passage;
- Thermal mixing zone determination; and
- Design optimization, reservoir/lake stratification, selective cold water withdrawal.

U^2RANS uses state-of-the-art, unstructured CFD technology, unifies multi-block structured mesh (quad or hex) and unstructured mesh (quad, triangle, tet, hex, wedge, pyramid, or hybrid) elements into a single platform, and combines 2D and 3D solvers in a common framework. A User's Manual is available, which

provides a more detailed description about the general features and capabilities (Lai, 2002). The major theory was also published as journal papers by Lai et al. (2003a,b).

Physical processes included in U^2RANS are as follows:

- Accurate solution of the Reynolds Averaged Navier-Stokes (RANS) equations for three-dimensional fluid flows through any solution domain with complex geometry;
- Several turbulence models within the RANS framework that allow 3D mesoscale features predicted, such as secondary flows at the meandering bends and point bars, vortex/eddy generation due to hydraulic structures, vertical flow characteristics, etc.; and
- Temperature and scalar transport simulated accurately using the energy and mass conservation equations.

3. Description of Study Site and Available Data

3.1 Model Domain

Two model domains are developed for the present study: low resolution and high resolution domains.

The low resolution domain covers about 115 km (69 miles) of the Sacramento River. It starts at Freeport (river mile 47.6) at the downstream and ends at Wilkins Slough (river mile 117) at the upstream; a map view of the domain is shown in Figure 2. The low resolution model domain covers the river section through the city of Sacramento, along the Fremont Weir, past Knights Landing, and towards Wilkin Slough just downstream of the Tisdale Weir. The model includes several tributaries: the Feather River and the American River. Laterally, the model domain covers both the main channel and the overbank area between the levees. The channel width above the Feather River confluence averages 85 meters while it is about 150 meters below the confluence. The bed slope over the model domain is fairly consistent and averages about 0.0082%. The bed material of the main channel contains predominately sand, with medium sediment diameter (d50) ranging from 0.2 to 0.4 mm (Hall et al., 2010).

The low resolution model was originally developed by Dynamic Solutions LLC (2011) who carried out a 2D modeling study using the ADH model. Their 2D model was initially calibrated against the 2002 flow data. It was then verified using the 2010 flow data. The same low resolution model was later updated by Hammack et al. (2013a) and the revised ADH model was used to simulate the flow period between December 12, 2010 and March 1, 2011.

The low resolution model developed by Hammack et al (2013a) is adopted by the present study. That is, the same model domain, 2D mesh, and boundary conditions are used without any changes. The 2D mesh consists of pure triangles as ADH can only use such a mesh; so the advantage of using the hybrid mesh by SRH-2D is not used. Only major difference between the present study and the Hammack et al. (2013a) study is that the present modeling used SRH-2D, not ADH. For reporting convenience throughout this report the SRH-2D low resolution model is named Low-Res-2D.

First, the Low-Res-2D model is used to simulate the flow period between December 8, 2010 and March 1, 2011; this serves as the model calibration study. The calibration simulation may be viewed as a repeat of the Hammack et al. (2013a) study except that SRH-2D model is used. The simulation results are compared with the available stage and discharge data observed at several gauges, the ADCP velocity data, and the ADH model results by Hammack et al. (2013a). Comparisons to the observed stage, discharge, and velocity serve as calibration of the model, while comparison to Hammack et al's (2013a) ADH modeling serves as the model verification. Once evaluated within the calibration period, the Low-Res-2D is further used to simulate the study's flow period of December 1, 2014 to March 31, 2015. This simulation serves as a second model validation study as model results may be compared with the available field data. The 2014-2015 Low-Res-2D model results are also used to provide boundary conditions for the fine resolution 3D model.

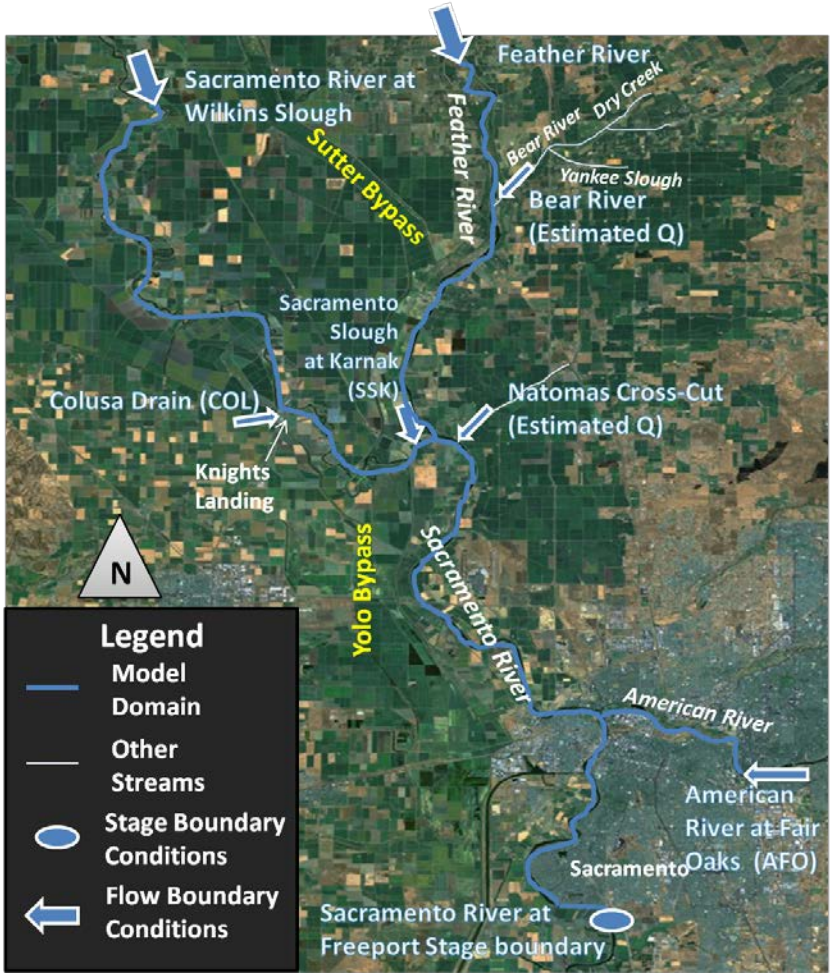

Figure 2. Low resolution model domain developed for the modeling of the Sacramento River (Dynamic Solutions, 2011)

The high resolution domain is developed in this study for 3D modeling using U^2RANS. It is named High-Res-3D for reporting purpose. The model domain is shown in Figure 3. The High-Res-3D model starts from Knight Landing at the upstream and ends at Verona gauge station at the downstream. The approximate longitudinal length of the model domain is about 18 km (10.8 miles). High-Res-3D model includes five open boundaries: Knights Landing inflow, Feather River inflow, Verona outflow, and small inflows from Sacramento Slough at Karnak and Natomas Cross-Cut. The boundary conditions at these five open boundaries are discussed later in the next chapter.

High-Res-3D model is used to simulate selected days during the period of December 1, 2014 and March 41, 2015 under the existing condition. The 3D modeling performed so far concentrates on model validation by comparing model results with the available stage, discharge and ADCP velocity data.

Figure 3. High resolution model domain used for U^2RANS modeling of the Sacramento River near Fremont Weir, the Sacramento River, California

3.2 Field Data

Two sets of field data are available for model calibration and validation.

The first data set corresponds to the period of December 2010 to March 2011. It is used primarily for SRH-2D model calibration. The data set includes the following:

- 2010/2011 flow and stage (water elevation) data at various gauge locations which are used for roughness calibration;
- 2010/2011 ADCP data at 42 river transects which are used to verify the model capability to predict flow velocities; and
- ADH model results, carried out by Hammack et al. (2013a), which are available for model comparison between different models.

The bathymetry of the Low-Res-2D model is based on a number of datasets between 1997 and 2000. A detailed discussion of these data sets was presented in the report of Hammack et al. (2013a) and not repeated herein. A brief presentation is made later in the model results section with regard to other data sets.

The second data set corresponds to the period of December 2014 to March 2015. These data were specifically collected for this project in order to carry out the U^2RANS 3D modeling. They are described in more details below.

The data include the following:

- 2015 bathymetric data at selected transects and longitudinal sweeps, which are used to develop the proper river model;
- 2014/2015 flow and stage (water elevation) data at some gauge locations in the period; and
- 2015 ADCP velocity data at ten transects at selected days of the period (to be described next for detailed locations).

The bathymetric data was collected by the Department of Water Resources (DWR), California for the 2015 Fremont Weir fish behavior Study; the data collection time is between January 21 and 27, 2015. The bathymetric data points from the survey are displayed in Figure 4. The data set covers about the last 10 km (6 miles) of the High-Res-3D model domain. The bathymetry upstream of the survey, about 8 km (4.8 miles), is based on the fine resolution ADH model developed and described by Hammack et al. (2013b) (terrain data was between 1997-2000). Further, the set of Lidar data surveyed on dry land in March and April, 2008 is available to represent the dry areas of model domain.

A composite, continuous terrain encompassing the High-Res-3D model domain, is developed by combining the 2015 bathymetric data, the upstream ADH fine resolution model terrain and the 2008 dry area Lidar data. The composite terrain is used to develop the 3D mesh for the High-Res-3D model. Data processing is carried out using both the Surface-water Modeling System (SMS) developed by the Aquaveo, LLC. and Reclamation terrain processing tools. The 2015 final composite terrain used is shown in Figure 5. As a comparison, the terrain used by

the ADH high resolution model of Hammack et al. (2013b) is shown in Figure 6. Visual comparison of the two terrains shows that the changes in terrain between 1997-2000 and 2015 are relatively small in the study area of the Sacramento River.

Figure 4. 2015 bathymetric survey spatial extent and data points

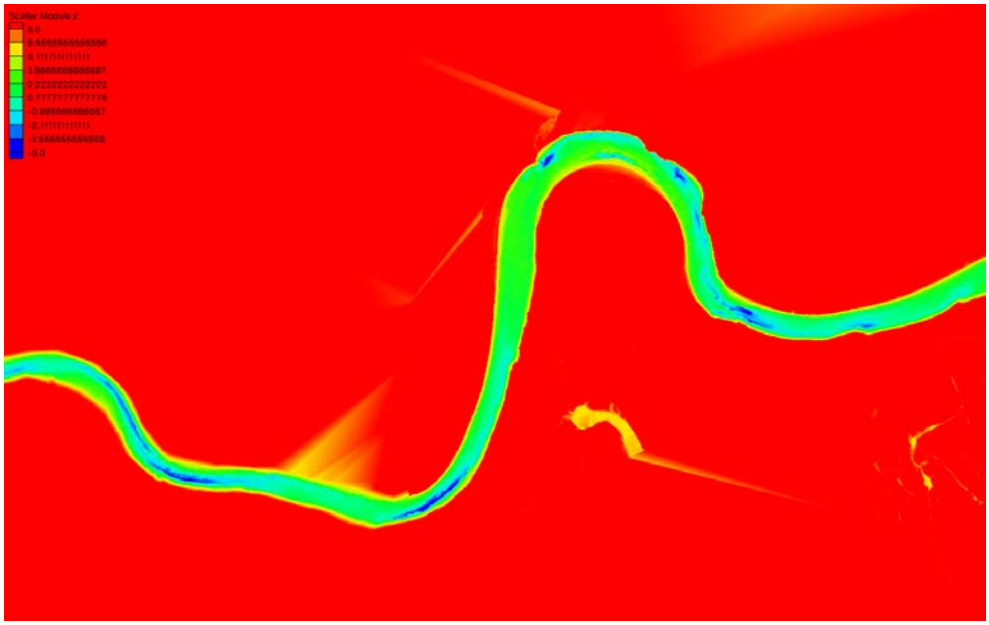

Figure 5. Bed elevation contours in the big bend area of the High-Res-3D model based on the 2015 survey data

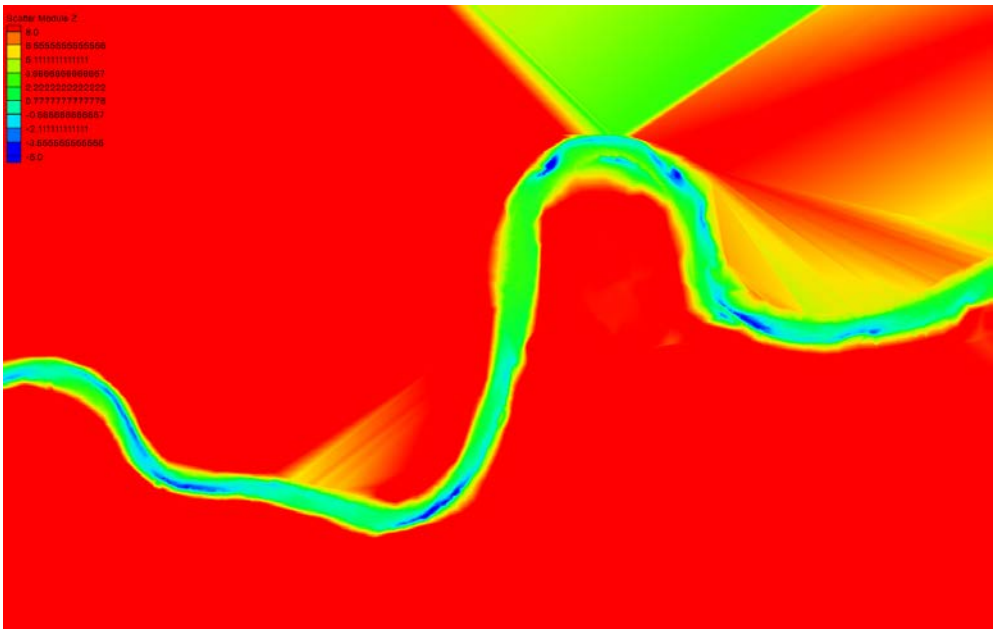

Figure 6. Bed elevation contours in the big bend area of the High-Res-3D model based on the 1997-2000 ADH high resolution model

4. Numerical Model Development

Both 2D and 3D numerical models have been developed to simulate flow hydraulics along the Fremont Weir area of the Sacramento River. In general, river flow modeling includes the following steps:

- Selection of the model domain;
- Mesh generation for the solution domain;
- Topography, flow roughness representation on the mesh and initial and boundary conditions;
- Model calibration and if applicable model verification; and
- Model application.

Step 2 and 3 are described below for the present study below. Step 1 was already discussed in Chapter 3.

4.1 Low Resolution Model

4.1.1 Mesh and Terrain

The Low-Res-2D model domain has been described in Chapter 3 and the domain is shown in Figure 2. The 2D mesh was originally generated with the SMS mesh generation software and provided to us through ERDC/USACE. Discussion on how the mesh and the bathymetry were developed is presented in model support and calibration reports (Dynamics Solutions 2011; Hammacks et al. 2013a). In summary, the 2D mesh consists of a total of 64,577 purely triangular cells and 35,023 nodes as shown in Figure 7. Close-up views of the mesh at the Fremont Weir area is shown in Figure 8.

The bed elevation of the Low-Res-2D model was based on the bathymetry and terrain data collected between 1997 and 2000 as part of the Sacramento-San Joaquin Basins River Comprehensive Study. Changes of the Sacramento River in planform and bed elevation were relatively small so the model was deemed adequate in simulating the flow in the period of 2010-2011 as documented by the USACE engineers (Hammacks et al. 2013a).

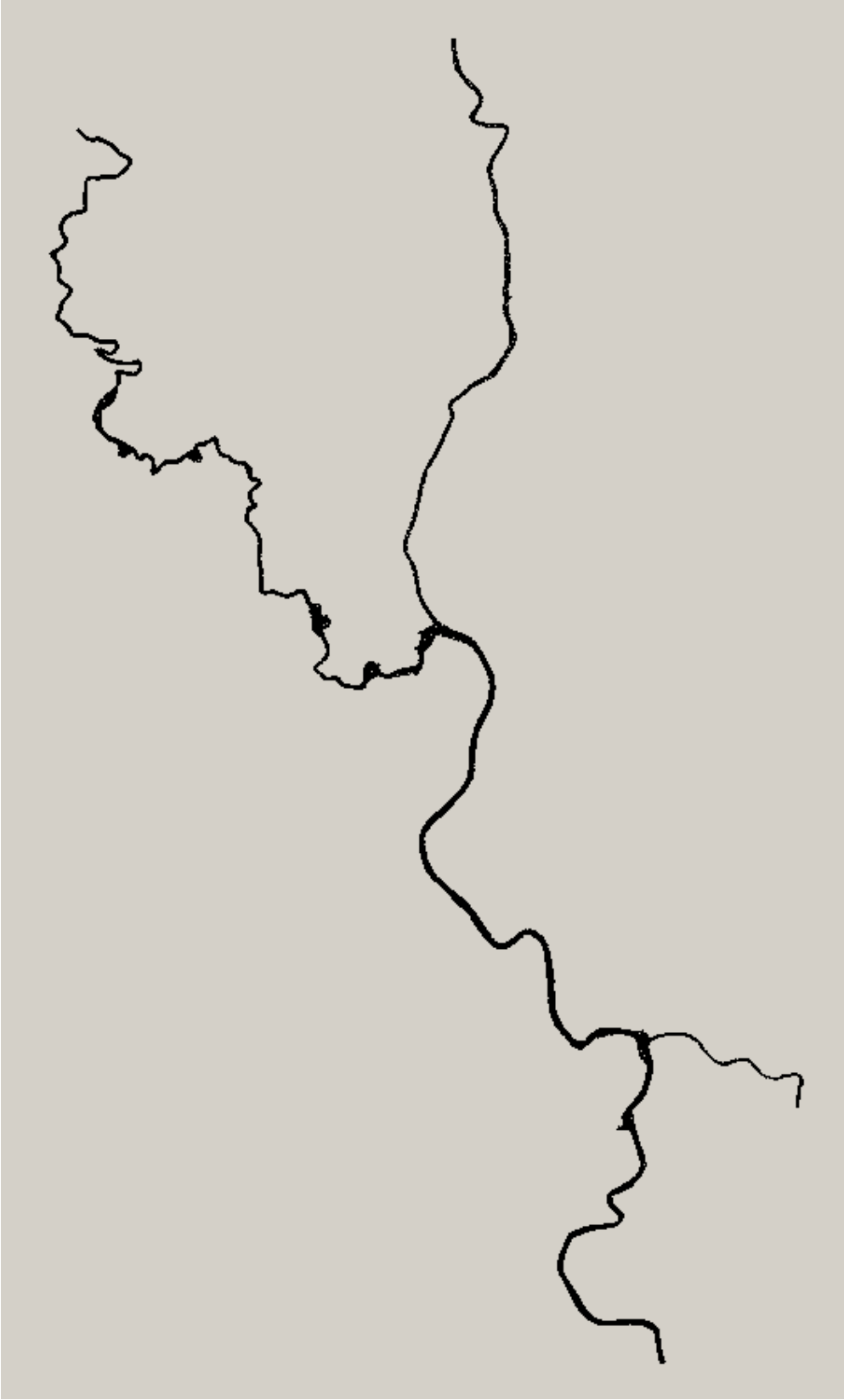

Figure 7. 2D mesh of the low resolution model domain: Overview

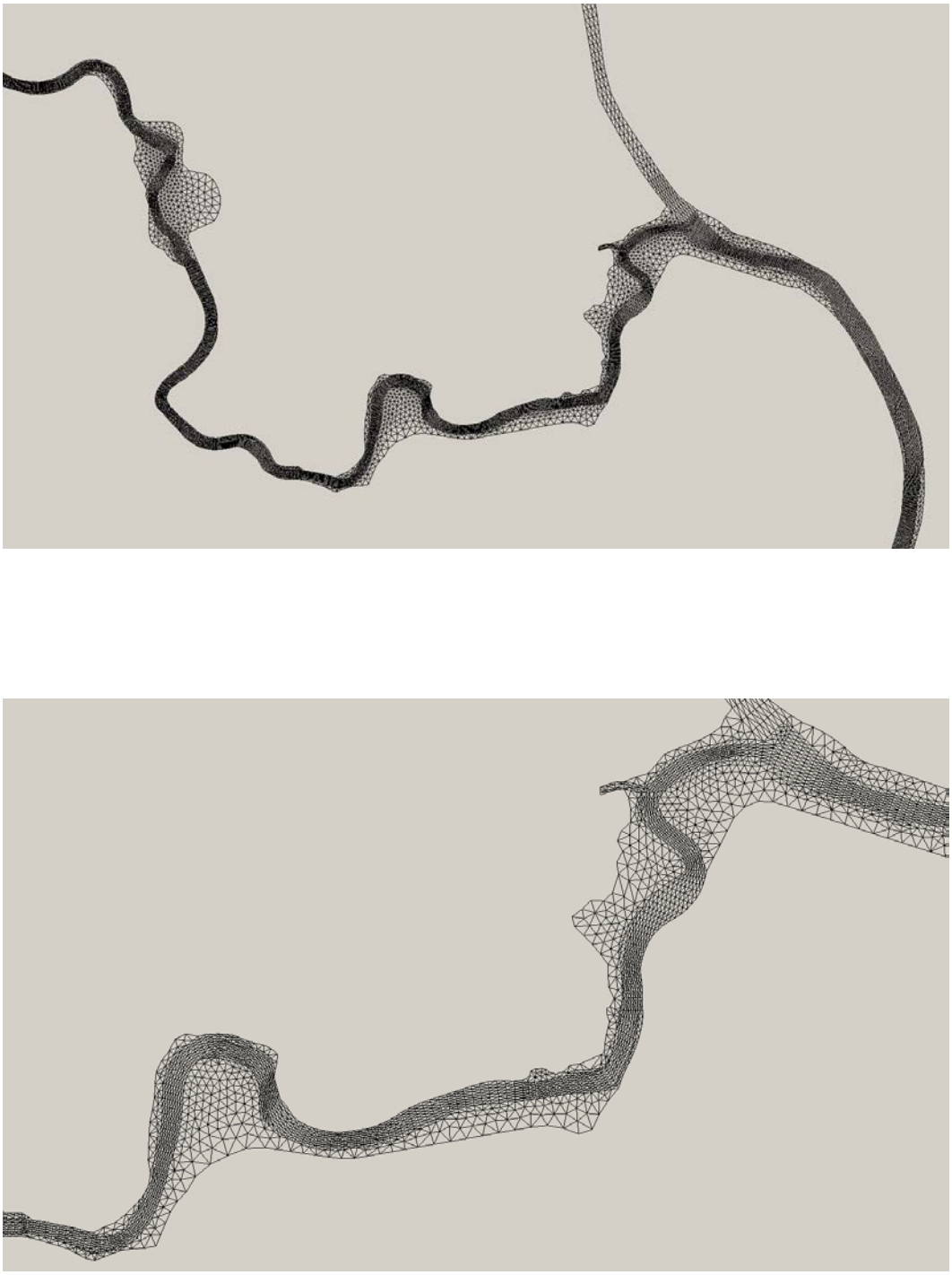

Figure 8. Close-up views of the 2D mesh for the Low-Res-2D model domain in the Fremont Weir area

4.1.2 Roughness Representation

Flow resistance is calculated with the Manning's roughness equation by SRH-2D (see Lai, 2008). The Manning's coefficient (n) is a model input and the primary calibration parameter of SRH-2D. The model domain is partitioned into 18 zones similar to Dynamic Solutions LLC (2011) ADH model and the Manning's coefficient in each zone was then calibrated by comparison model results with the gauge discharge and stage data. The same 18-zone partition as the ADH model is used by the present study and the Manning's coefficient is then determined through a calibration process. Initially, the same manning's coefficients as those calibrated by Hammack et al. (2013a) for ADH are used. Then, several more model runs are performed using smaller and larger Manning's coefficients than the ADH values. The final calibrated Manning's roughness coefficients for SRH-2D are determined based on the comparison of model results with the gauge data of discharge and stage. The n-values used by the present study are 10% higher than those used by ADH. The 18 roughness zones are displayed in Figure 9 and Figure 10; while the calibrated n-values used by SRH-2D are in Table 1. It is not obvious why the Manning's coefficients used by SRH-2D are 10% higher than those by ADH. It is conjectured that the use of different turbulent viscosities may play an important role. Differences in numerical discretization and algorithms may also be important as the 2D mesh is very coarse.

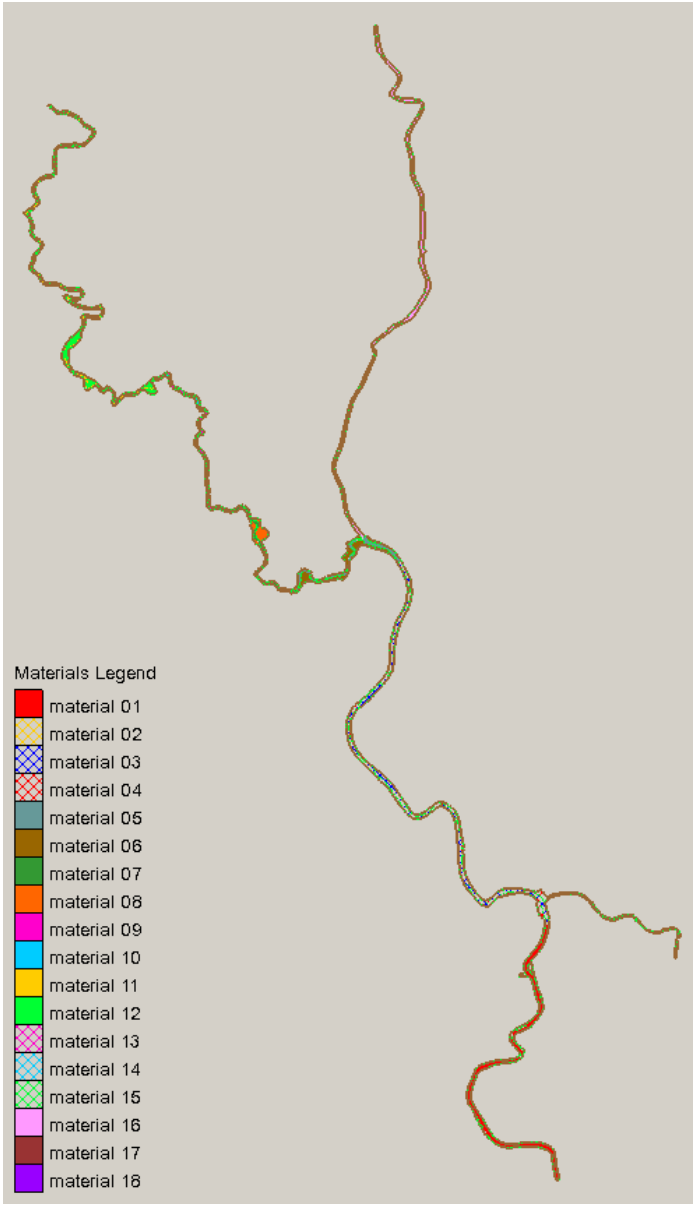

Figure 9. Eighteen zones of the Manning's roughness coefficient for the Low-Res-2D model: entire model domain

Figure 10. Zones of the Manning's roughness coefficient in Freemont Weir area

Table 1. Manning's coefficients used by Low-Res-2D model within 18 zones

ID	1	2	3	4	5	6
Location	main channel downstream of American	overbank downstream of American	main channel between American and Feather	overbank between American and Feather	main channel along Freemont Weir	overbank along Freemont Weir
n	0.0286	0.044	0.0264	0.0495	0.02365	0.0495
ID	7	8	9	10	11	12
Location	main channel between Freemont and Knights Landing	overbank between Freemont and Knights Landing	main channel of lower section from Knights to Wilkins	overbank of lower section from Knights to Wilkins	main channel of upper section from Knights Landing to Wilkins	Overbank of upper section from Knights to Wilkins
n	0.0231	0.0495	0.0264	0.055	0.0264	0.055
ID	13	14	15	16	17	18
Location	Sacramento and American Confluence wetland	Sacramento and American Confluence wetland	American River	Feather River	Sacramento Slough at Karnak	Colusa Drain entrance
n	0.033	0.033	0.033	0.0242	0.0242	0.0242

4.1.3 Boundary Conditions

There are a total of eight open boundaries of the Low-Res2D model – seven discharge boundaries and one stage boundary (refer to Figure 2 for their locations). The discharge and stage data at these eight locations are obtained mostly from gauge records and a few are estimated. A detailed description of each gauge station and how the data were assembled together were provided by Hammack et al. (2013a). Only a summary is provided below.

The upstream boundary of the Sacramento River is at the Wilkins Slough at river mile 117.5; discharge data is from the USGS gage 11390500. The hourly discharge hydrograph is used by the model. It is shown in Figure 11 for the period of December 12, 2010 to March 1, 2011, and Figure 13 for the period of December 1, 2014 – March 31, 2015.

The downstream boundary of the Sacramento River is at Freeport, which is influenced by the tide propagation from San Francisco Bay through the Delta. The tidal influence is not negligible particularly during the low flow season. Stage data is obtained from the USGS Freeport gauge 11447650. The record is plotted in Figure 12 for the December 12, 2010 - March 1, 2011 period and in Figure 14 for the December 1, 2014 – March 31, 2015 period.

A major tributary inflow to the Sacramento River is the Feather River, which joins the Sacramento at river mile 80. A section of the Feather River was added to the model domain to avoid estimation of the discharge into the Sacramento River and to take into account the tidal influence. The upstream boundary of the Feather River is at Boyd's Landing where a CA DWR station (CDEC station FBL) provides the discharge data (see Figure 11 and Figure 13 for the two periods simulated). The Bear River flows into the Feather River just above the junction with the Sutter Bypass and was also taken into the model. The discharge from the Bear River is estimated from a combination of the Bear River gage near Wheatland (USGS 11424000), the Dry Creek gage (USGS 11418500), and the Yankee Slough tributaries between the gage and the confluence. The discharge from the Bear River is shown in Figure 11 and Figure 13 for the two periods.

A 10 km (6 miles) section of the American River was included as a tributary inflow to the Sacramento River in the city of Sacramento and to take the tidal signal propagation into account. Flow hydrograph is obtained from the Fair Oaks gage (USGS 11446500) and displayed in Figure 11 and Figure 13 for the two simulated periods.

Other inflows to the model domain include: (a) flow into the Sacramento River from the Sutter Bypass, 800 meters upstream of the Feather River confluence, via the Sacramento Slough near Karnak (flood flow condition is not considered when the entire Sutter Bypass is flowing); (b) flow from the Natomas Cross-cut, downstream of the Feather River confluence but above the Verona gage, which is estimated to be 30% of the Bear River flow; and (c) Colusa Basin drainage canal into the Sacramento River adjacent to the western edge of the town of Knights Landing. The discharge data of the Sutter Bypass at Karnak and the Colusa Basin had the recorded data for the period of Dec 12, 2010 - March 1, 2011, but not for the period of December 1, 2014 – March 31, 2015. In this study, they are found to be in significant and will be discussed in the results section.

Note that the potential flow over the Fremont Weir, at river mile 83.5 and with a crest of 10.21 m (33.5 feet and NAVD88), to the Yolo Bypass is not considered by the model. The operation of the Fremont Weir is not accounted for by the model either. Other small inflows enter into and pumping occurs within the solution domain; but they are not considered. Adjustments to the gage discharges are used to achieve the flow balance.

Several additional gauges are available to check and calibrate the model. For example, the Verona flow and stage gauge (USGS 11425500) at river mile 78.5 and the Fremont Weir (West) stage gauge (CA DWR A02170) are available for model calibration.

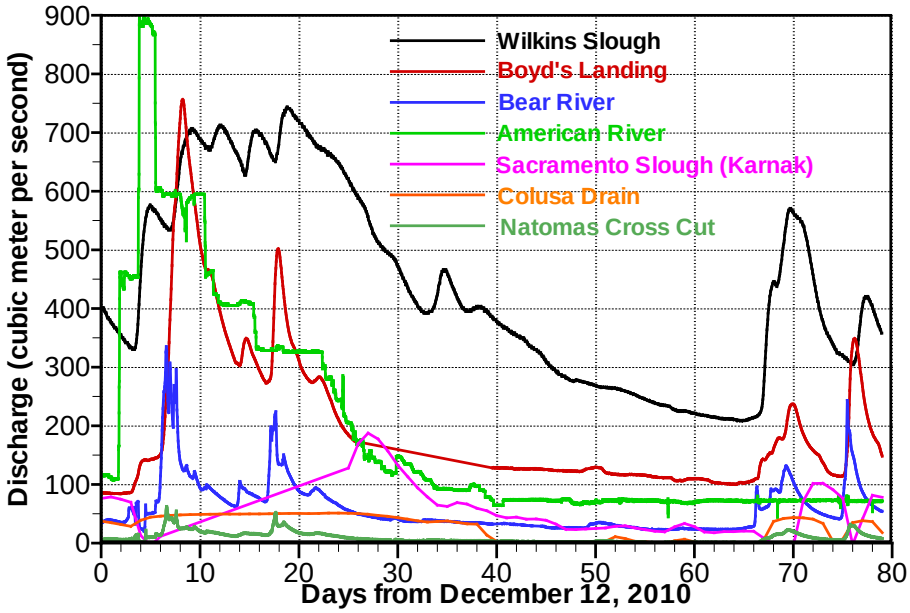

Figure 11. Flow hydrographs at seven inflow boundaries of the Low-Res-2D model from December 12, 2010 to March 1, 2011

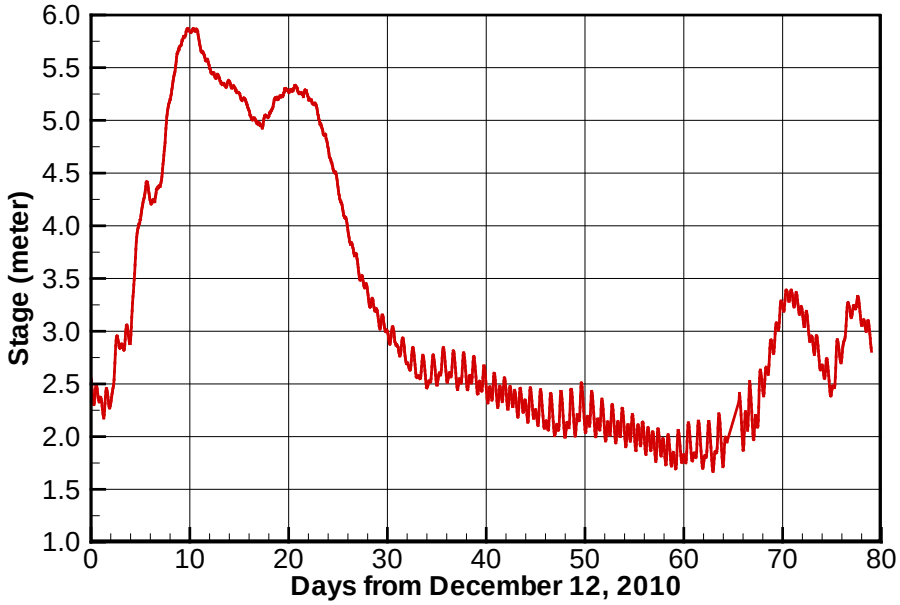

Figure 12. Stage recorded at the Freeport for the Low-Res-2D model from December 12, 2010 to March 1, 2011

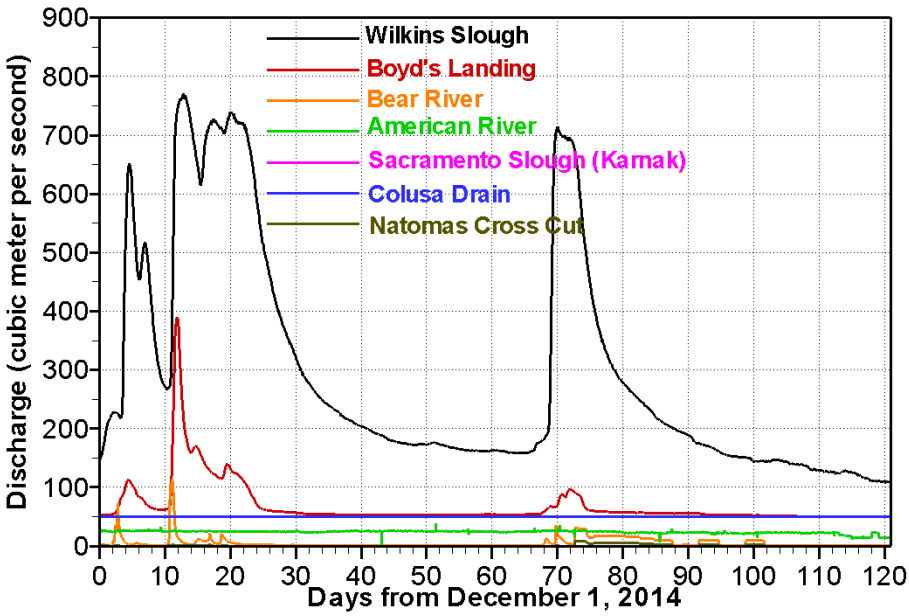

Figure 13. Flow hydrographs at seven inflow boundaries of the Low-Res-2D model from December 1, 2014 to March 31, 2015

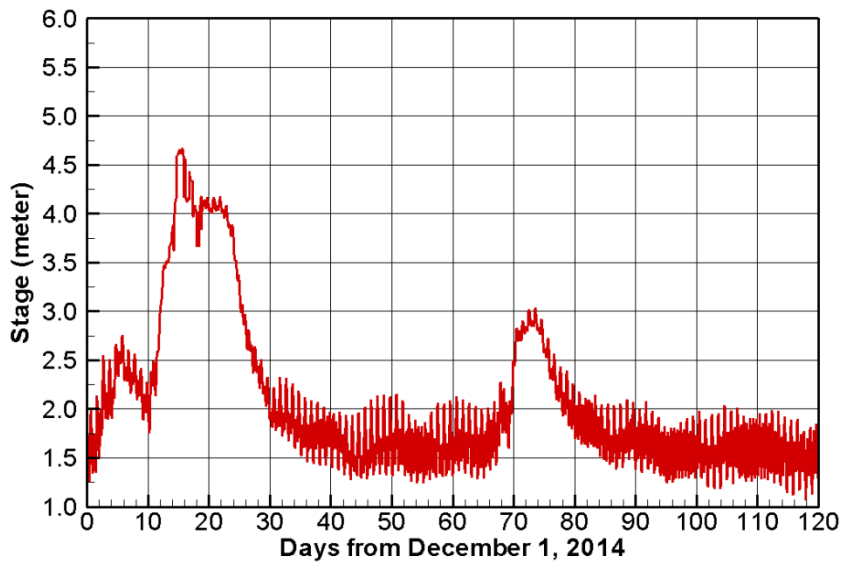

Figure 14. Stage recorded at Freeport for the Low-Res-2D model from December 1, 2014 to march 31, 2015

Table 2. Stations used to develop the boundary conditions (Source: Dynamic Solutions, 2011)

Name	Type	Data Source	Gage	Abbreviation
Freeport	Downstream Stage	USGS	11447650	FPT
American River at Fair Oaks	Discharge	USGS	11446500	AFO
Calusa Drain near Knights Landing	Discharge	CA DWR	A02945	COL
Sacramento Slough at Karnak	Discharge	CA DWR	SSK	SSK
Wilkins Slough	Upstream Discharge	USGS	11390500	WLK
Feather River at Boyd's Landing	Discharge	CA DWR	FBL	FBL
Bear River near Wheatland	Discharge	USGS	11424000	N/A
Deer Creek near Smartville	Discharge	USGS	11418500	N/A

4.2 High Resolution Model

The high resolution model, High-Res-3D, has a model domain about 18 km (10.9 miles) in length as described in Chapter 3 and shown in Figure 3; it is developed for U^2RANS 3D modeling. The model results under the existing condition are obtained so that they are compared with the ADCP data for model validation. The numerical results are used as inputs to the ELAM model for fish movement simulation and for comparison with the telemetry fish tracking data. In the next phase, the High-Res-3D model will be extended to include the Fremont Weir area and the potential alternative weir notch designs so that the effect of the notch on local flow hydrodynamics may be predicted, compared and evaluated.

4.2.1 Mesh and Terrain

The mesh for the High-Res-3D is developed in two stages. First, a 2D mesh is obtained covering the model domain using SMS. An overview and two close-up views of the mesh are shown in Figure 15 through Figure 17. This 2D mesh consists of 35,701 mesh cells of mixed quadrilaterals and triangles (7,444 triangles and 28,257 quadrilaterals). The mesh is used for SRH-2D modeling to provide the initial condition for the U^2RANS modeling. Next, the 3D mesh is developed using either the sigma-mesh approach carried out automatically by U^2RANS or the sophisticated mesh generator snappyHexMesh. The results from both meshes are found to be very close. With the sigma-mesh, a total of 20 vertical cells are used resulting in a total of 714,020 3D mesh cells comprising both hexahedrons and prisms. The 3D mesh has been developed under the existing condition without considering the Fremont Weir area as well as the weir notch design. The current model is used primarily for model validation by comparing results with the ADCP data and to provide flow inputs to the ELAM model for fish movement modeling.

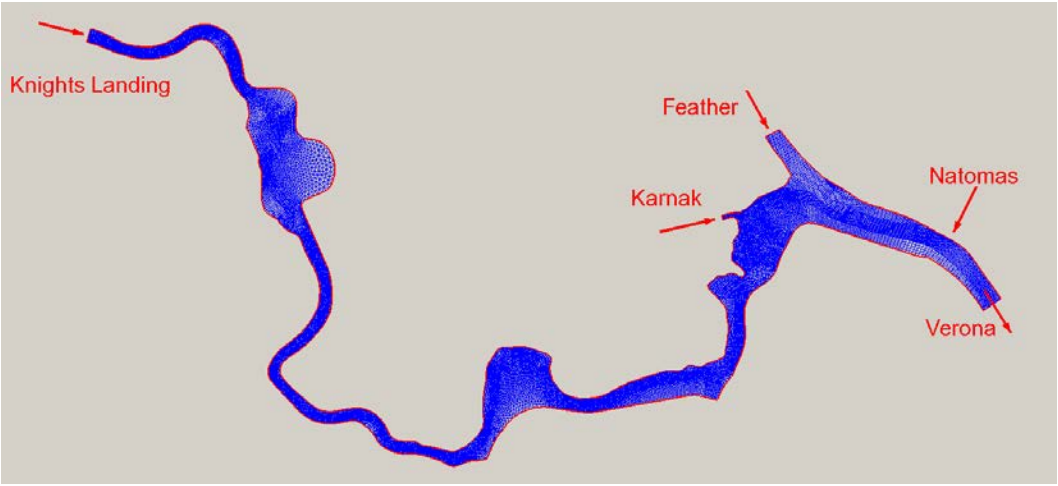

Figure 15. An overview of the 2D mesh developed for the High-Res-3D model

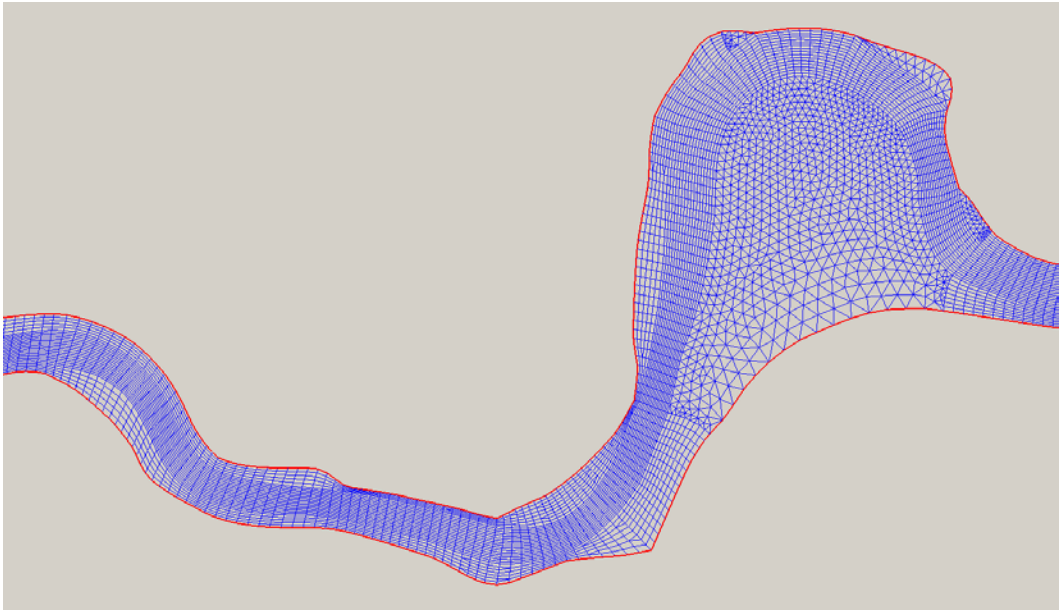

Figure 16. A close-up view of the High-Res-3D mesh at the big bend area of the Fremont Weir section

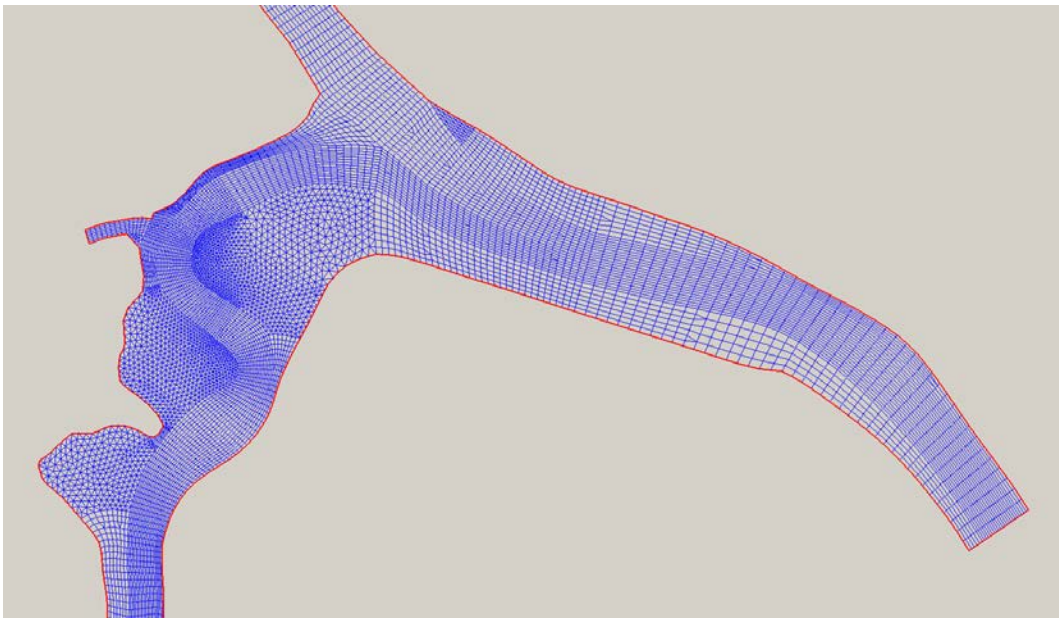

Figure 17. A close-up view of the High-Res-3D mesh at the confluence of the Sacramento River and the Feather River

The High-Res-3D model is primarily developed to simulate the 2014-2015 period so the 2015 bathymetric data in the model area are used (see discussion in Chapter 3). The 2015 terrain was interpolated onto the High-Res-3D mesh so that the 3D mesh may represent the river accurately. The terrain represented by the 3D mesh is shown in Figure 18. 3D close-up views of the terrain at the big bend area of the model are displayed in Figure 19 and Figure 20.

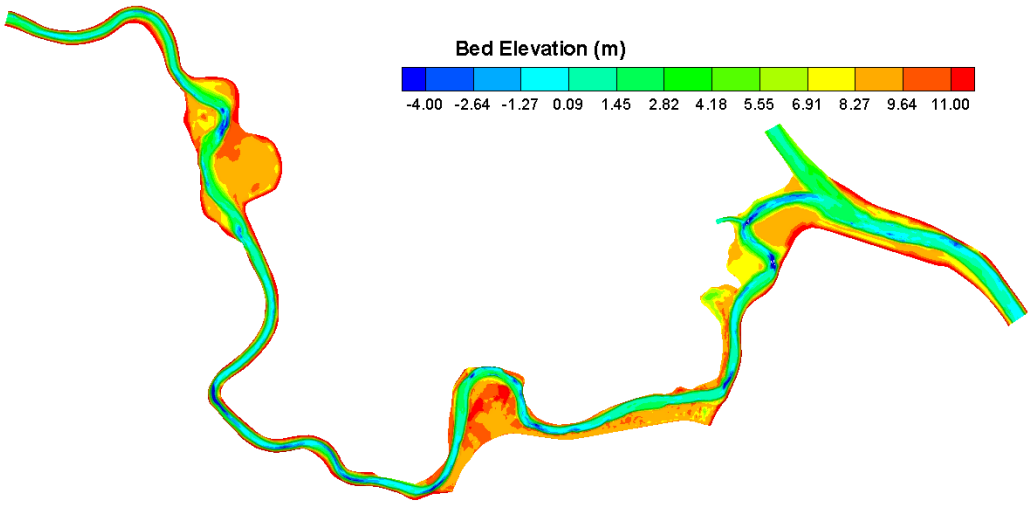

Figure 18. 2015 terrain represented by the High-Res-3D mesh: entire domain view

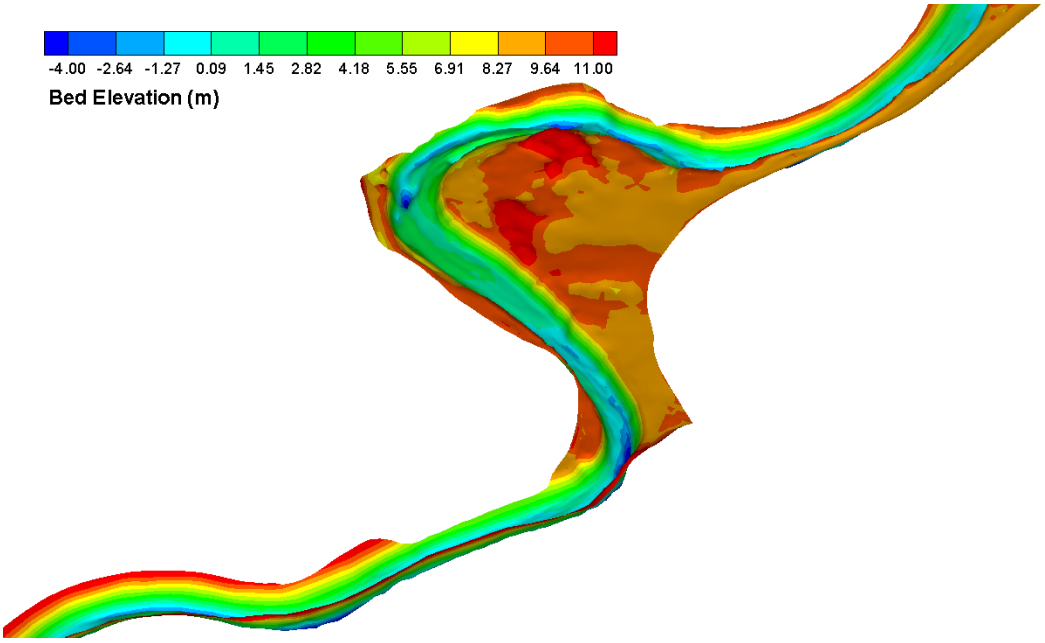

Figure 19. 2015 terrain represented by the High-Res-3D mesh: the upstream section at the big bend area (1:5 vertical distortion)

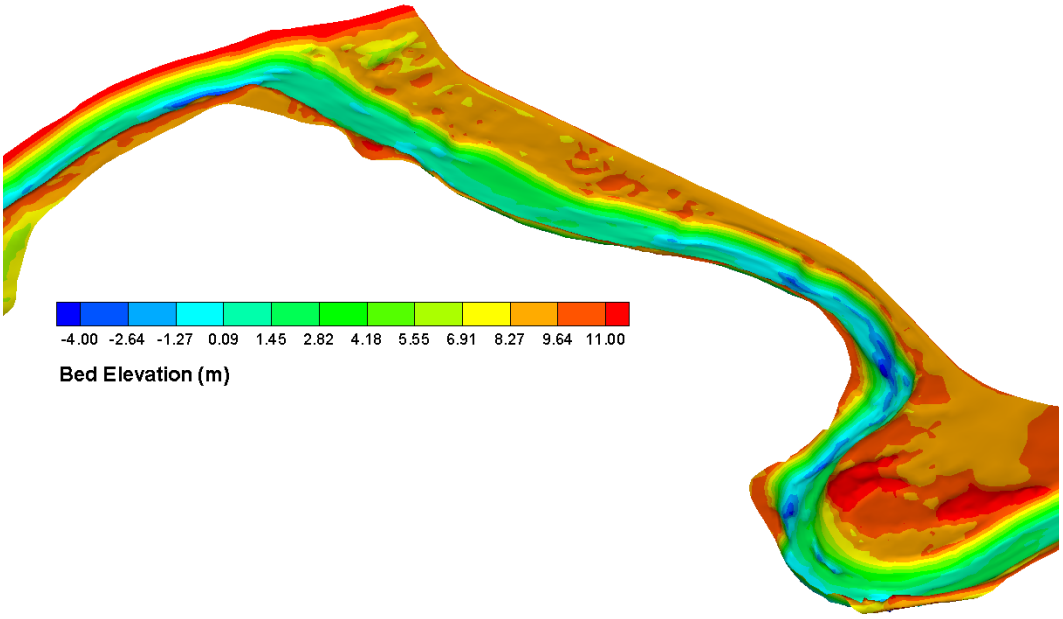

Figure 20. 2015 terrain represented by the High-Res-3D mesh: the downstream section of the big bend area (1:5 vertical distortion)

4.2.2 Boundary Conditions

There are five open boundaries that need boundary conditions for the High-Res-3D model (see Figure 3). They are discussed next.

At the upstream (Knights Landing), the flow discharge is originally taken from the Low-Res-2D model results for the period of December 2014 to March 2015. Simulated model results, however, show that the discharges predicted by the Low-Res-2D model are much lower than the gauge data indicates (see discussion in Chapter 5). Therefore, it is decided that the discharge at Knights Landing is estimated using the discharge at Verona gauge, subtracted by the discharges at the Feather River, Natoma boundary and Karnak Slough. Such derived discharge is shown in Figure 21 and it is used as the upstream boundary condition at the Knights Landing.

For the 3D modeling, the above approach is accurate for low flows. For high flows such as on February 11, 2015, the estimated discharge through the Fremont Weir area is over-estimated. It is conjectured this model inconsistency is due to an under-estimate of the flow in the Feather River. Adjustment is made for the 3D modeling on February 11, 2015 as discussed later in Chapter 5.

The Feather River flow into the Sacramento River is based on the Low-Res-2D model for the period of December 1, 2014 and March 31, 2015. The flow hydrograph such obtained is shown also in Figure 21. As discussed above, the modeled flow in the Feather River may be under-estimated during high flow.

Other boundary condition to the Sacramento River with the High-Res-3D model include: those from the Sutter Bypass, 800 meters upstream of the Feather River confluence, via the Sacramento Slough near Karnak, and from the Natomas Cross-cut downstream of the Feather River confluence but above the Verona station. The Natomas flow is estimated to be 30% of the Bear River flow and is found to be very small and insignificant to the model results. The flow hydrographs from the Karnak Slough and the Sutter Bypass are the same as the Low-Res-2D model and they are shown in Figure 13.

Finally, the stage (water elevation) at Verona is based on the recorded gauge data and it is used at the downstream boundary condition. The stage data is plotted in Figure 22 for the period of December 1, 2014 to March 31, 2015.

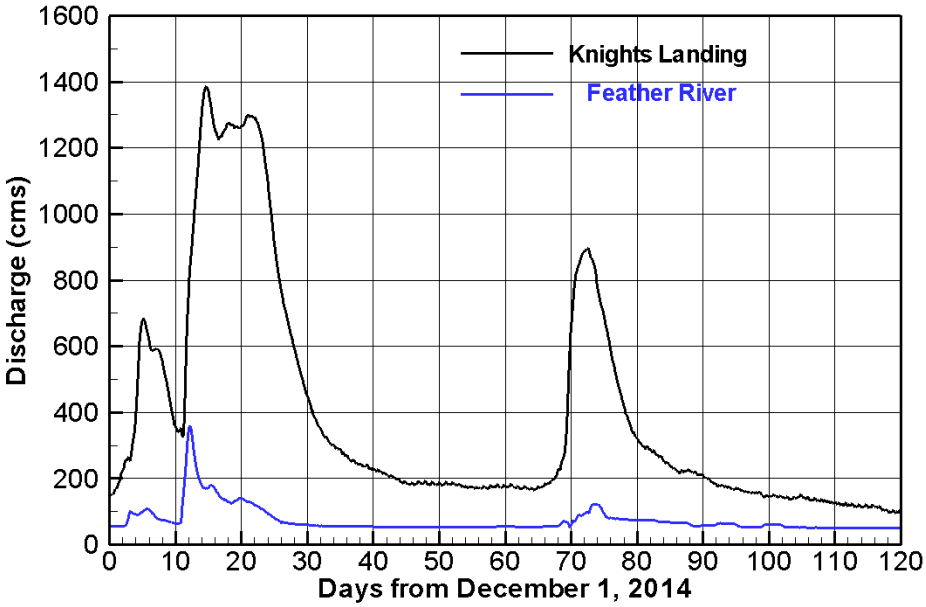

Figure 21. Flow discharges at the Knights Landing and Feather River for the period of December 1, 2014 to march 31, 2015

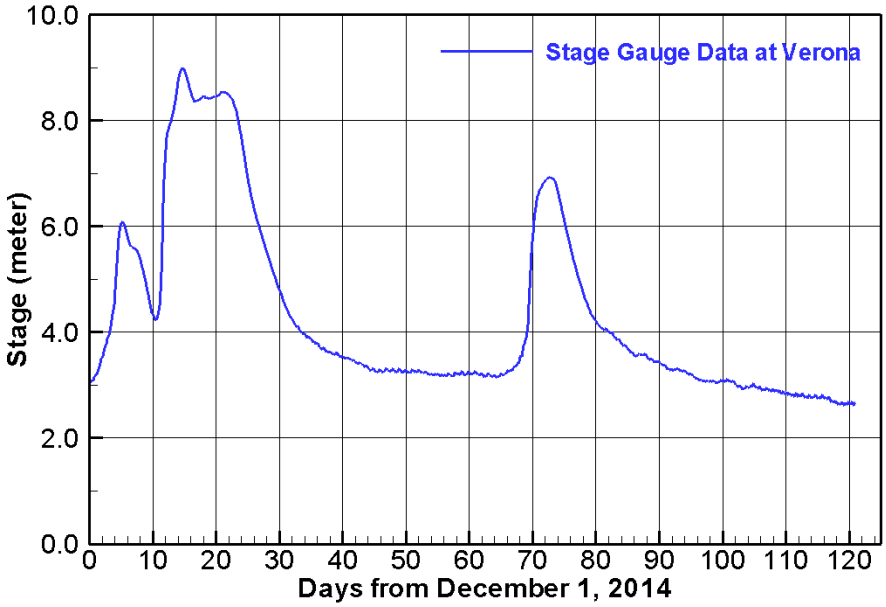

Figure 22. Stage at Verona gauge for the period of December 1, 2014 to March 31, 2015

5. Low Resolution 2D Model Results

2D simulation with the Low-Res-2D model is carried out first for the period of December 12, 2010 – March 1, 2011. This is referred to as the calibration study as the simulation intends to calibrate the 2D model using the available field data. The same model is further carried out for the period of December 1, 2014 to March 31, 2015. This serves as the model verification and the results are used to supplement the missing boundary condition of the High-Res-3D model.

5.1 Calibration Study

Flow and stage data at five gauges are used for Low-Res-2D model calibration to determine the appropriate Manning's coefficients. The five gauges are shown in Figure 23 and summarized in Table 3.

In addition, the ADCP velocity data are available at 42 river transects between river miles (RM) 80 and 87 during January 31 - February 2, 2011. The model results are compared with the ADCP data to verify the accuracy of the model in velocity prediction.

Further, the same simulation was performed previously by Hammack et al. (2013a) using the ADH model. The current SRH-2D model results may also be compared with ADH.

Only the Manning's roughness coefficient is the primary recommended calibration parameter with SRH-2D. Other modeling parameters, such as the turbulence model and diffusion/dispersion coefficients, are not calibrated and they assume the suggested default values. A total of 18 zones are used to represent the Manning's roughness coefficient (see Figure 9 and Figure 10). With the parabolic turbulence model selected, our first model run is to start with the Manning's coefficients in the 18 zones determined by Hammack et al. (2013a) with the ADH. A number of additional model runs are then carried out by a percentage increase and decrease in the Manning's coefficient. The appropriate values of the Manning's coefficient are determined by comparing the model results with the gauge stage and discharge data. Our final Manning's coefficients are calibrated to be 10% higher than the ADH model used by Hammack et al. (2013a) and they are listed in Table 1. Readers may refer to Hammack et al. (2013a) for a detailed discussion on how they carried out their calibration.

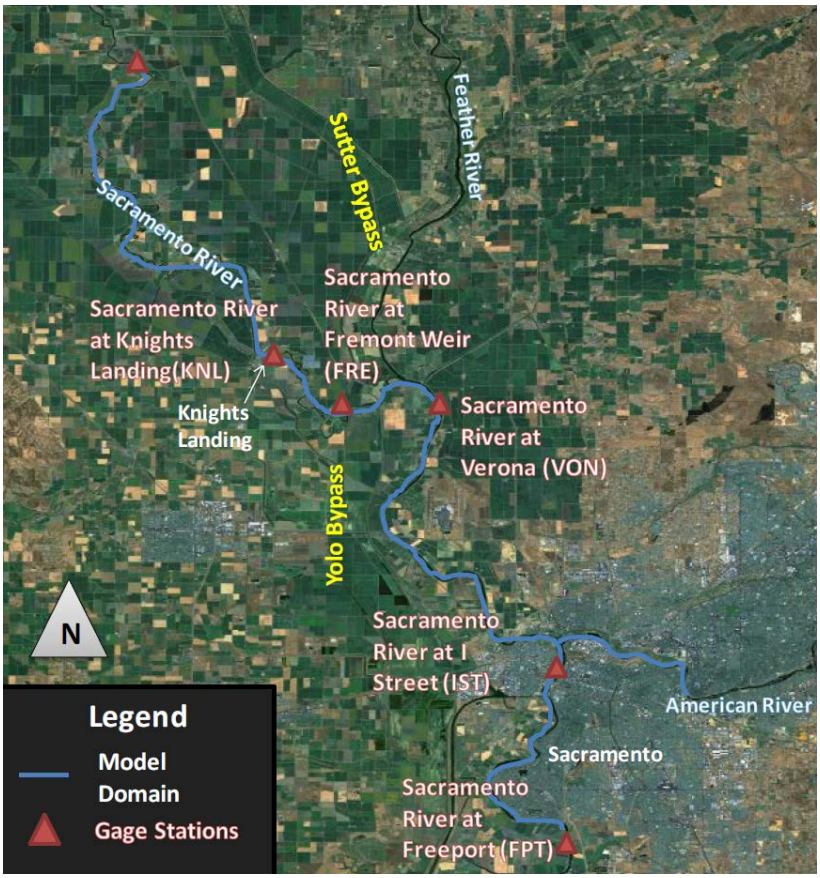

Figure 23. Gauge locations for Low-Res-2D model calibration (Dynamics Solutions, 20110)

Table 3. Sacramento River gauges used for model calibration

Gage Name	Data Type	Data Source	Gage Designation
Freeport	Discharge	CDEC	FPT
I Street Bridge	Stage	CDEC	IST
Verona	Discharge & Stage	CDEC	VON
Fremont Weir (West)	Stage	CA DWR	A02170
Knights Landing	Stage	CADWR	A02200

Comparisons of the calibrated Low-Res-2D model results and the recorded data at five gauges are reported next. The simulated water surface elevation (stage) is compared with the recorded river stages in Figure 24 through Figure 27 at four gauges. The four gauges are (from downstream to upstream): I-Street bridge,

Verona, Fremont Weir, and Knight's Landing. The results labeled as Low-Res-ADH are from the ADH and provided to us by USACE engineers.

The comparison shows that SRH-2D model results match very well with the ADH results. This is important since both models claimed to have been well verified and have been used widely for numerous project applications over the years. SRH-2D and ADH solve the same governing partial differential equations (PDEs) but use quite different numerical discretization schemes and solution algorithms. The comparison offers another test case verifying that both models meet the "consistency" property that their discretized equations recover to the PDEs they intend to solve.

The numerical model results compare well with the river stage data except for the high flow period. At the highest flow stage, both SRH-2D and ADH underpredict the stage by up to 1.5 m. This discrepancy was attributed to a number of causes by Hammack et al. (2013a). Potential causes include insufficient model resolution, unverified gauge data, or insufficient friction definition when the river stage is high. We conjecture that the mesh resolution is not the primary cause, as a very fine resolution model does not improve the comparison. Increased friction along banks at high flows may help improve the comparison but might be a secondary cause. We suspect that either the discharge data at some gauges have high uncertainty during high stage flow period or there are unaccounted in- and out-flows through the model domain. For example, the flow at Wilkin Slough is the only major inflow into the model domain through the Fremont Weir section of the Sacramento River. If there are more inflows into the Sacramento River between Wilkin Slough and Fremont Weir, the predicted stage may rise up to match the recorded stages at all four gauge stations.

One use of the Low-Res-2D model results is to supply boundary conditions to the High-Res-3D model. The above results show that the predicted stage of the Low-Res-2D model is inappropriate to use in the Fremont Weir area during high stage flow. We, therefore, decide to place the downstream boundary of the High-Res-3D model at the Verona gauge station so that the directly measured stage is used as the downstream boundary condition.

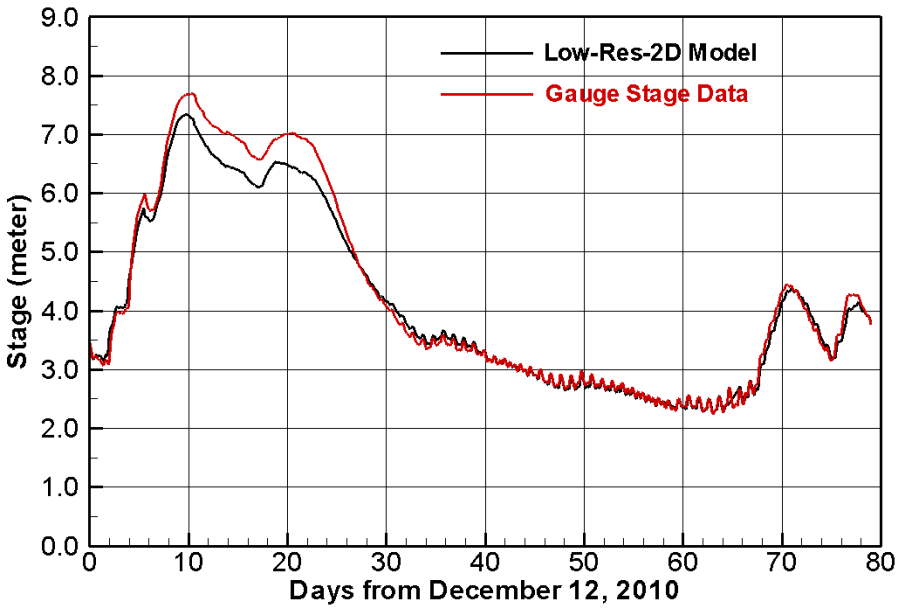

Figure 24. Comparison of simulated and recorded stage at I-Street Bridge gauge between December 12, 2010 and March 1, 2011

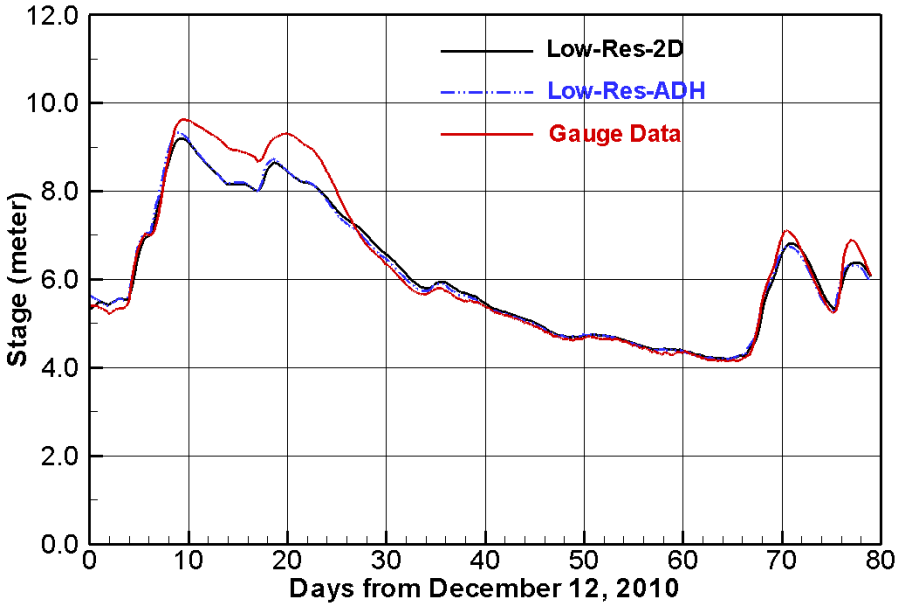

Figure 25. Comparison of simulated and recorded stage at Verona gauge between December 12, 2010 and March 1, 2011

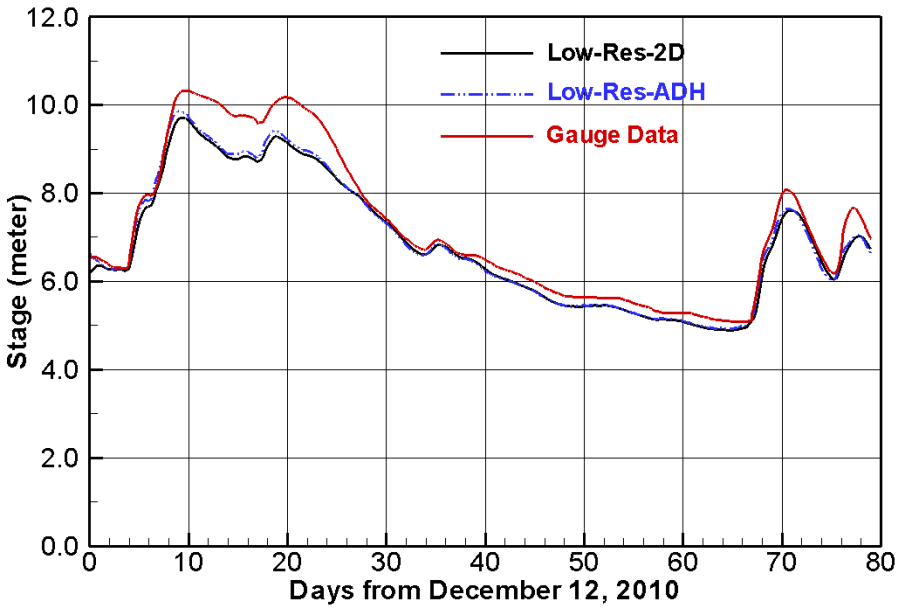

Figure 26. Comparison of simulated and recorded stage at Fremont Weir gauge between December 12, 2010 and March 1, 2011

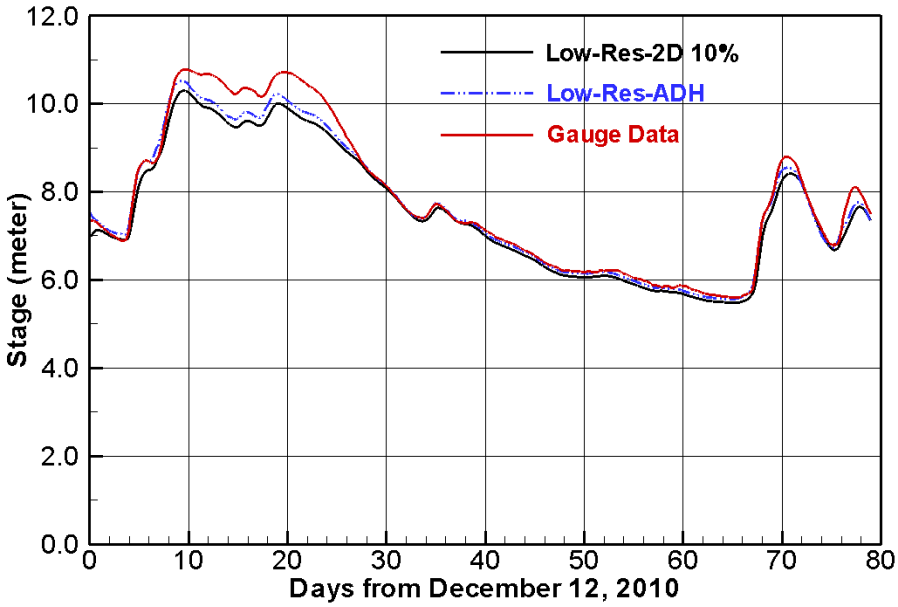

Figure 27. Comparison of simulated and recorded stage at Knight's Landing gauge between December 12, 2010 and March 1, 2011

The discharge simulated by the Low-Res-2D is compared with gauge data at Freeport and Verona in Figure 28 and Figure 29. The SRH-2D model results agree with the ADH model but both models underpredict the discharge at Verona significantly during high stage flow period (up to about 280 cubic meters per second). This discrepancy is consistent with the stage comparison due probably to the fact that not all inflows and outflows have been taken into account by the model at high flows. High flow through the Fremont area is of particular interest for the objective of this study, the discharge predicted by the Low-Res-2D model at the upstream boundary (Knights Landing) of the High-Res-3D model may be inadequate to use. Alternative way to specify the upstream discharge boundary condition for the Hogh-Res-3D model is needed and will be discussed later in Chapter 6.

It is noted that tidal influence on the discharge and stage at the Freeport gauge station is very significant at low stage flow period and the numerical models are capable of predicting such influence as shown in Figure 28. The tidal influence is insignificant at upstream locations such as at the Verona gauge station, at least for the simulated time period (Figure 25 and Figure 29).

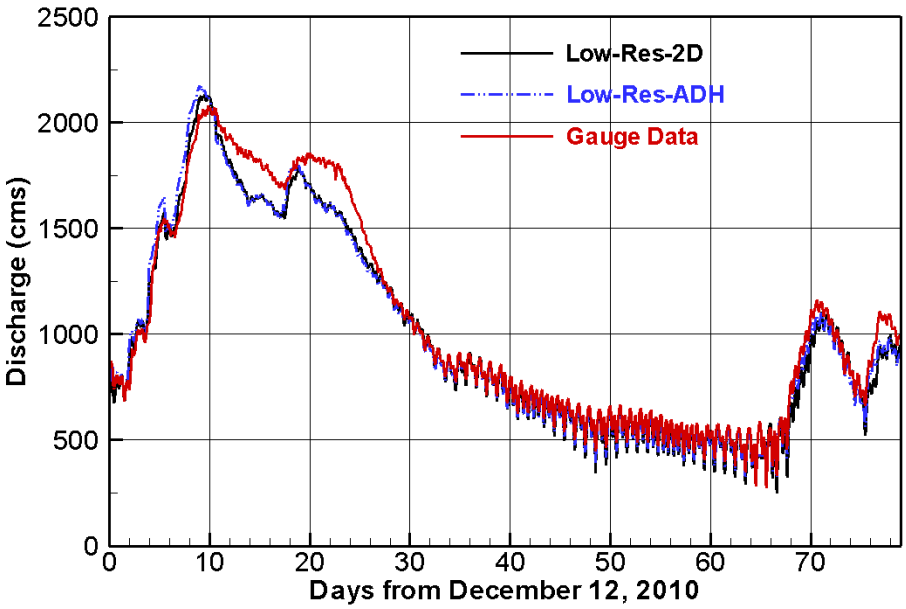

Figure 28. Comparison of simulated and recorded discharge at Freeport gauge between December 12, 2010 and March 1, 2011

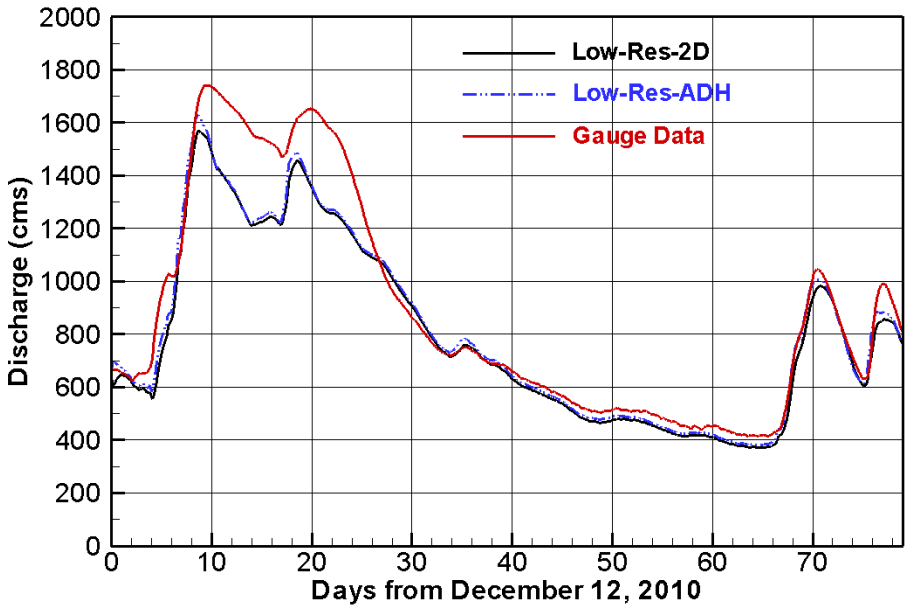

Figure 29. Comparison of simulated and recorded discharge at Verona gauge between December 12, 2010 and March 1, 2011

ADCP velocity data were collected between January 31 - February 2, 2011 at a section within the model domain and they are used to check how well the model can be used to predict the velocity in the river. The ADCP data was available on 42 transects between river miles (RM) 80 and 87 with a closer spacing between RM 85-86. The transects were spaced at 91 m (300 ft) in one section of the river and 321 m (1,056 ft) outside the section. The locations of these ADCP transects are shown in Figure 30 as white colored dots.

The raw ADCP velocity data was processed using two separate methods: incremental averaging and depth-averaging. The depth-averaged velocities allow for the most head-to-head comparison with the numerical model because depth-averaged velocities are directly calculated by SRH-2D. A total of 634 depth-averaged velocity points, located on the 42 transects, were available for comparison with the numerical model.

Figure 30. ADCP transect locations within the study area with white colored dots representing transects (Hammack et al, 2013a)

The ADCP measurement was carried out while the river stage was relatively low. The discharge at the Wilkin Slough gauge ranged from 263 to 269 cubic meters per second in the period of January 31 – February 2, 2011. The numerical model results on January 31 are extracted to compare with the ADCP data at all 42 transects. The depth-averaged velocity comparison is shown in Figure 31 through Figure 40 for all transects. A detailed statistical comparison is yet to be carried out. But a visual inspection of the comparison show that the SRH-2D predicted velocity is in general agreement with the ADCP data at most transects except for a few locations. Velocity comparison is much harder than the stage and discharge as velocity is a local flow variable and is influenced significantly by the local bathymetric features. Any bathymetric features which are not represented well by the terrain model can alter the velocity prediction. The overall good comparison of the predicted and ADCP velocity is very encouraging considering that a very coarse mesh has been used for the Low-Res-2D model. This point has been discussed in detail by Hammock et al. (2013a).

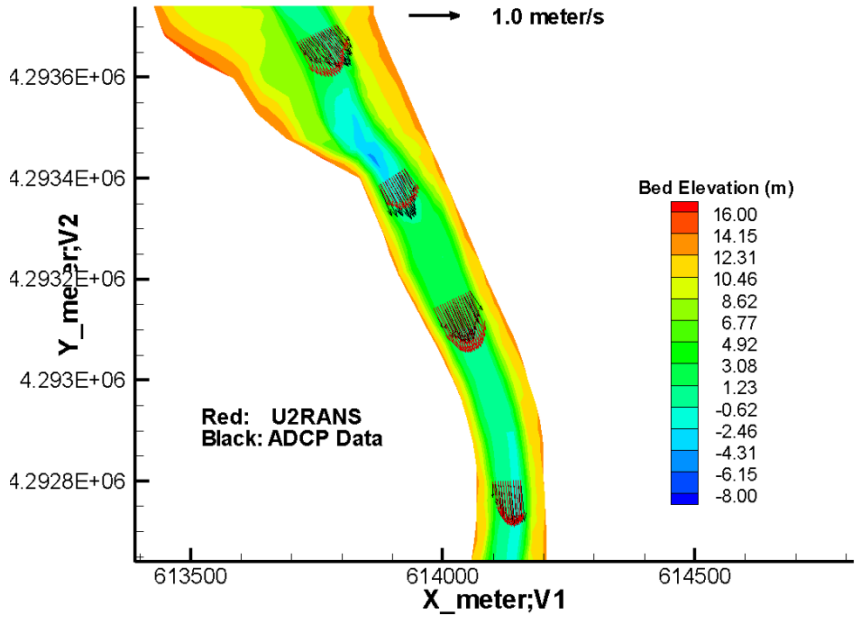

Figure 31. Depth-averaged velocity comparison on Transects 1 to 4 between Low-Res-2D and ADCP data

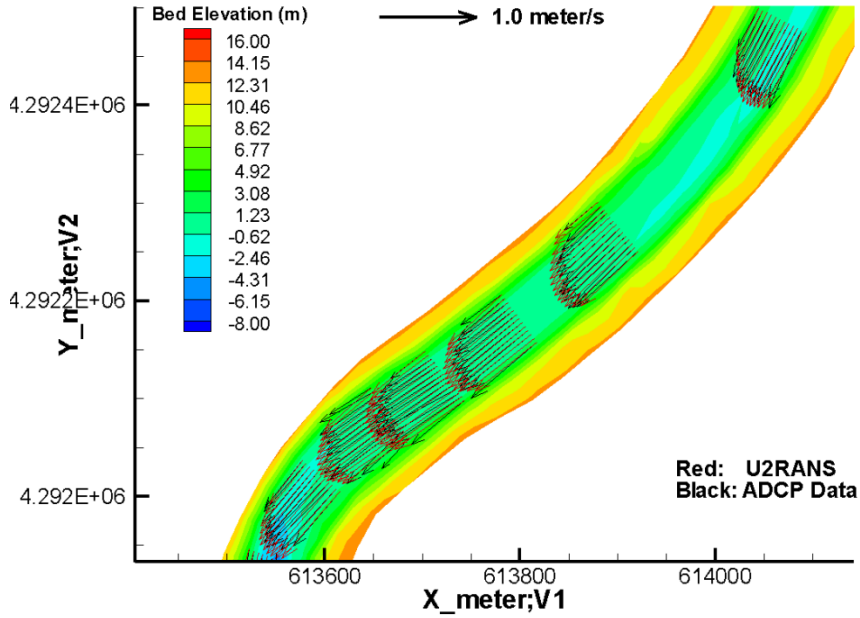

Figure 32 Depth-averaged velocity comparison on Transects 5 to 10 between Low-Res-2D and ADCP data

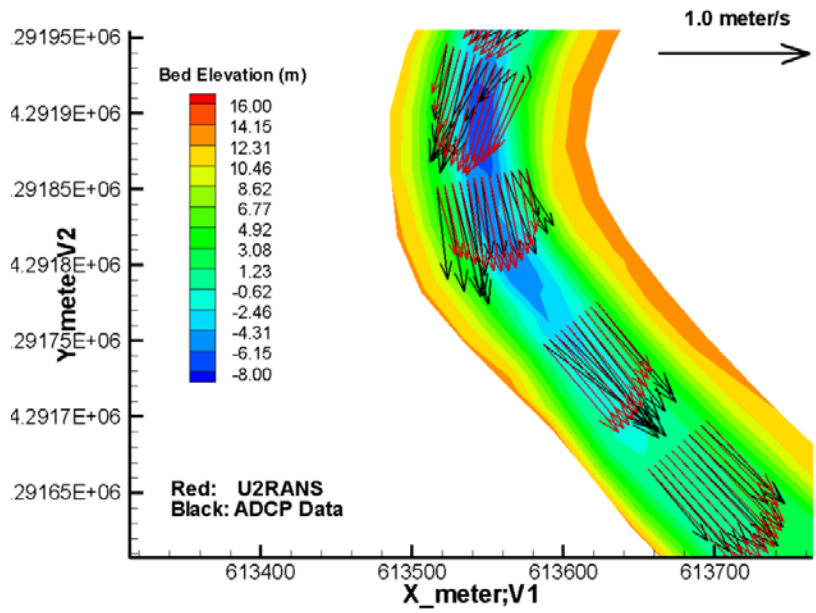

Figure 33. Depth-averaged velocity comparison on Transects 11 to 14 between Low-Res-2D and ADCP data

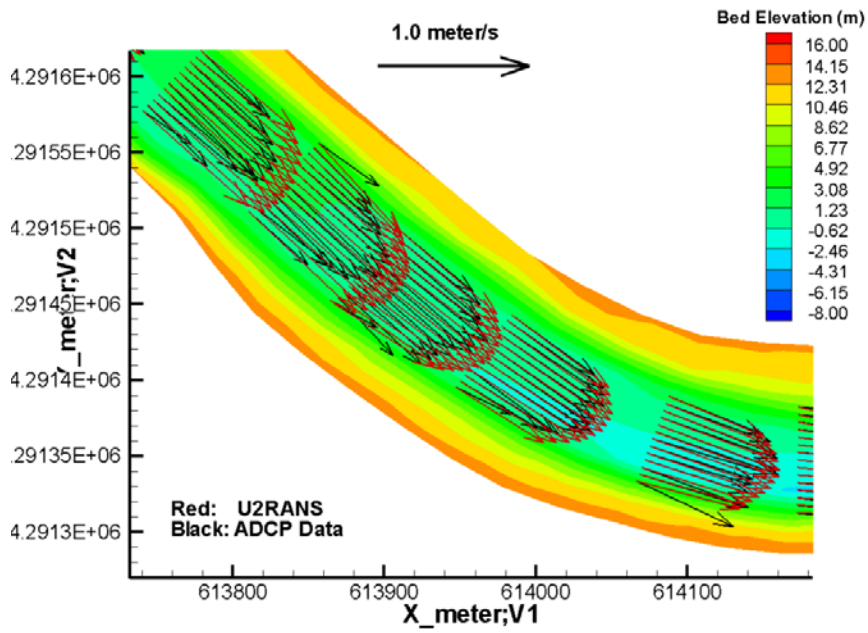

Figure 34. Depth-averaged velocity comparison on Transects 15 to 19 between Low-Res-2D and ADCP data

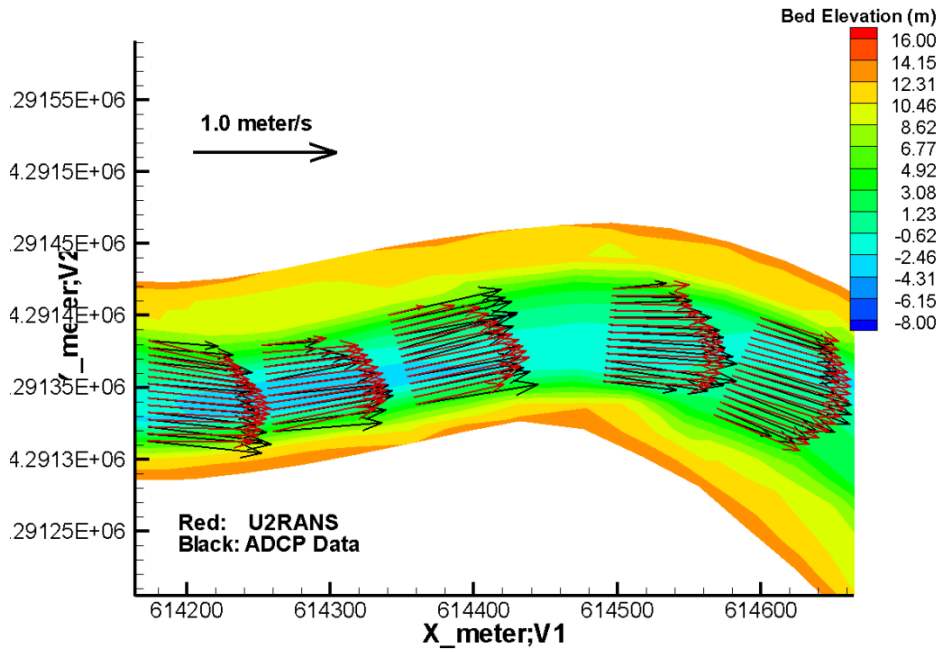

Figure 35. Depth-averaged velocity comparison on Transects 20 to 24 between Low-Res-2D and ADCP data

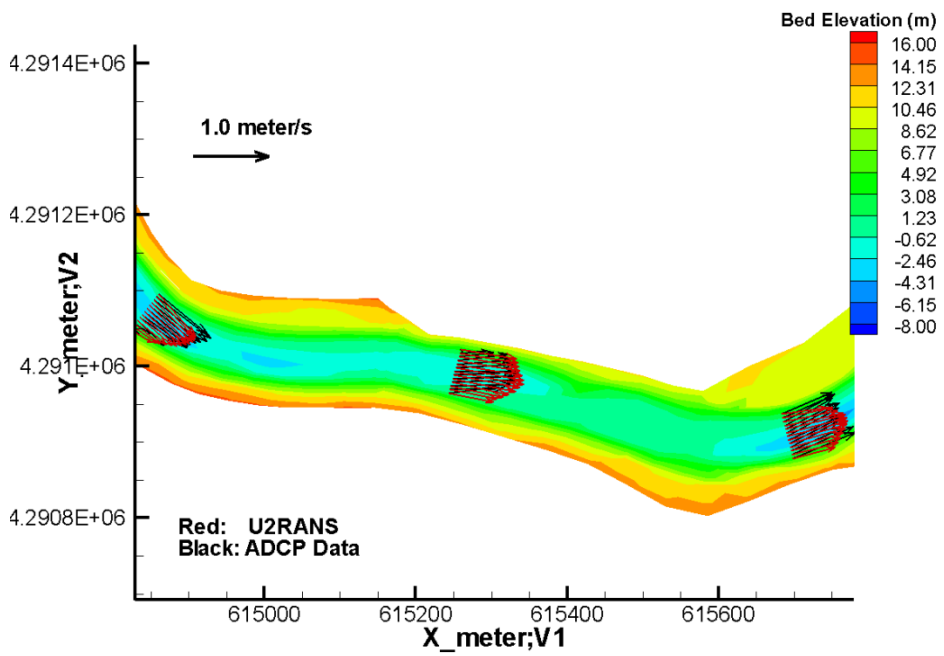

Figure 36. Depth-averaged velocity comparison on Transects 25 to 27 between Low-Res-2D and ADCP data

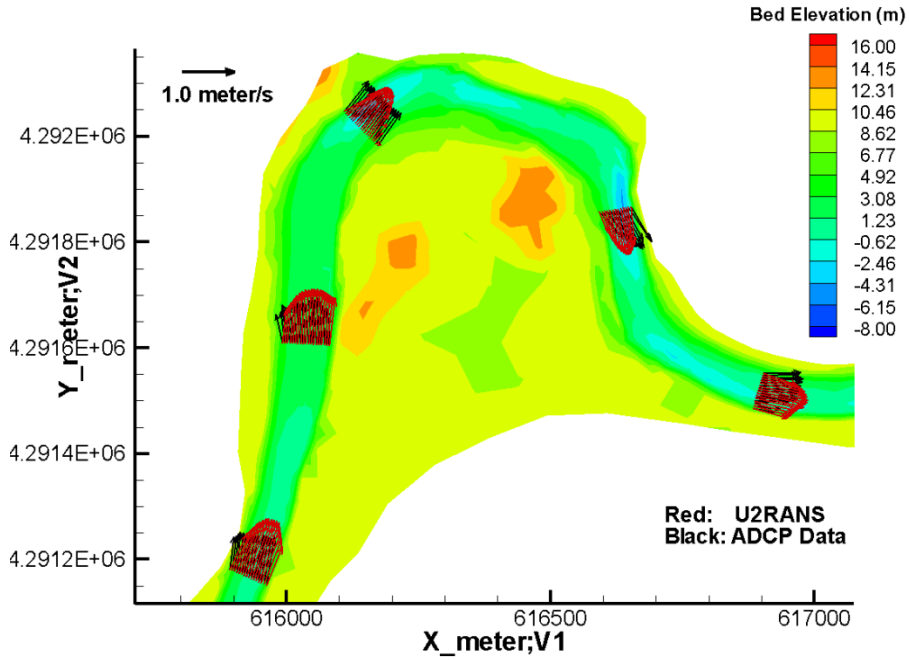

Figure 37. Depth-averaged velocity comparison on Transects 28 to 32 between Low-Res-2D and ADCP data

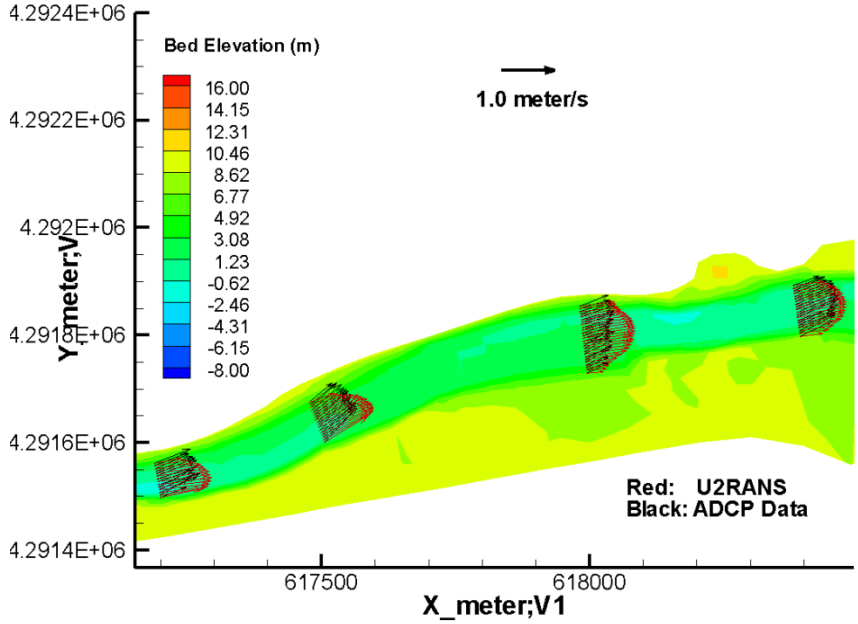

Figure 38. Depth-averaged velocity comparison on Transects 33 to 36 between Low-Res-2D and ADCP data

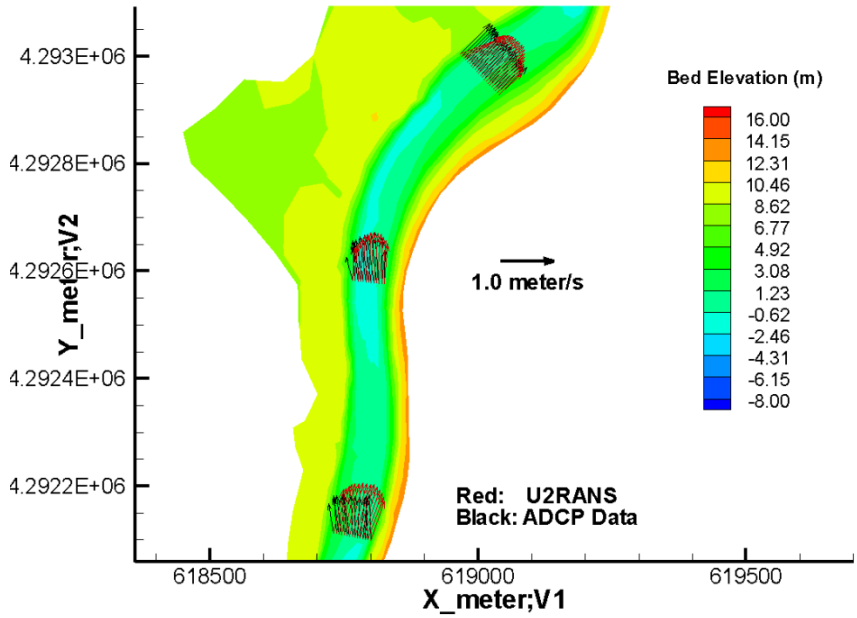

Figure 39 Depth-averaged velocity comparison on Transects 37 to 39 between Low-Res-2D and ADCP data

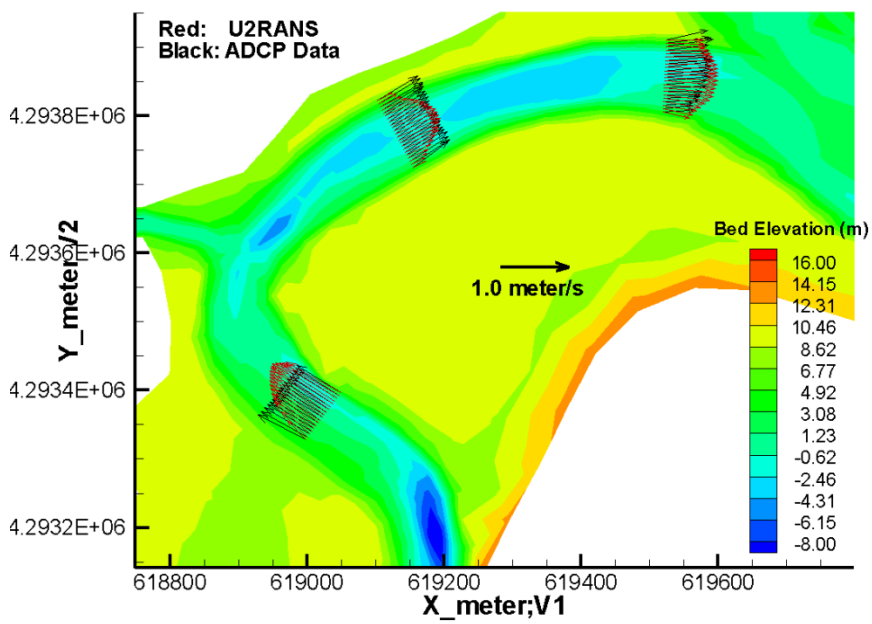

Figure 40. Depth-averaged velocity comparison on Transects 40 to 42 between Low-Res-2D and ADCP data

5.2 Verification Study

The same Low-Res-2D model is applied to simulate another time period between December 2014 and March 2015 without any changes to the model. The simulation serves as two purposes: for model verification and for providing the missing boundary conditions for the High-Res-3D model. Since the model is not recalibrated, the calibrated model is used as a predictive tool for other time periods. With the second field dataset available, a comparison of the model results with the data can be made to verify the model in that the model does not predict significantly different results in comparison with the data.

New boundary conditions are used corresponding to the flow and stage data recorded during December 2015 and March 2015 at gauges of all open boundaries (see discussion in Section 4.1.3). The simulation is then carried out for the time period. The predicted stage is compared with the recorded river stage at four gauge stations in Figure 41 through Figure 44 (They are listed from downstream to upstream: I-Street Bridge, Verona, Fremont Weir, and Knight's Landing). The comparison shows that model results behave very similarly to the calibration period of December 2010 – March 2011 in Figure 24 through Figure 27. That is, the model results agree well with the gauge data during most of the low flow periods but the model significantly underpredicts the stage during high flows. At the highest stage, the model underpredicts the stage by as much as 2 meters. As discussed in the calibration study section, the discrepancy at high flows is probably caused by high uncertainty of the discharge data at some gauges and unaccounted in- and out-flows within the model domain.

The discharges predicted by the model are compared with the Freeport and Verona gauges in Figure 45 and Figure 46. The model predicted discharge is as much as 400 cubic meters per second below the peak at the two gauges. This again shows that not all flows in the model domain have been taken into consideration by the numerical model.

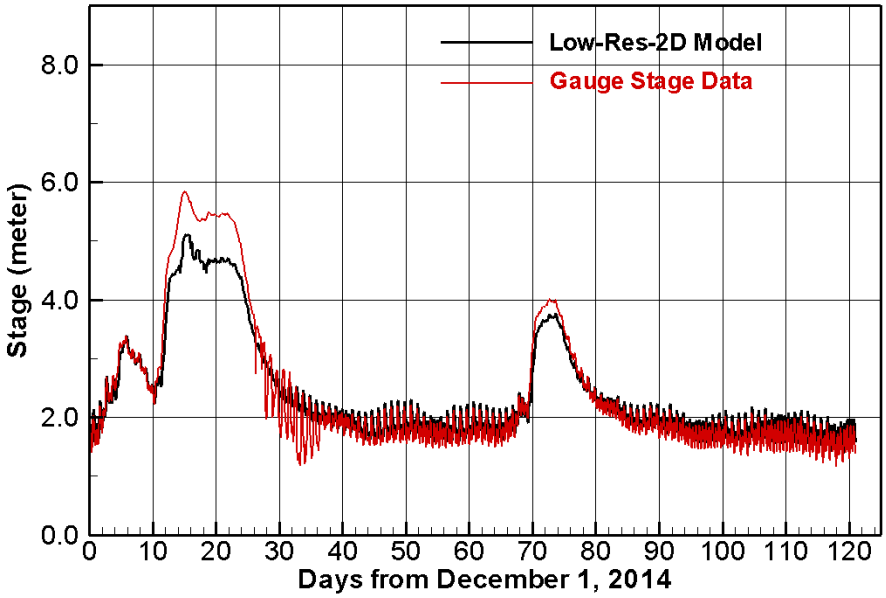

Figure 41. Comparison of simulated and recorded stage at I-Street Bridge gauge between December 1, 2014 and march 31, 2015

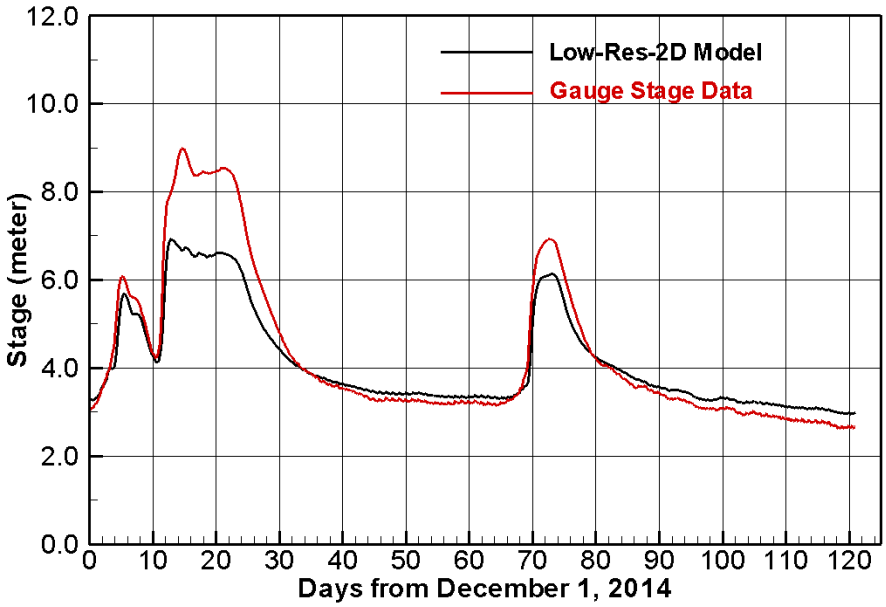

Figure 42. Comparison of simulated and recorded stage at Verona gauge between December 1, 2014 and March 31, 2015

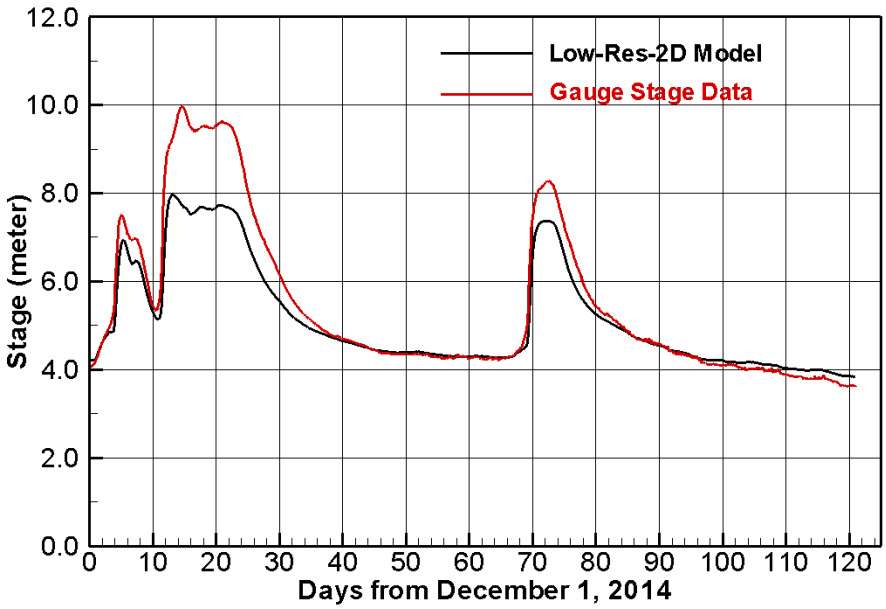

Figure 43. Comparison of simulated and recorded stage at Fremont Weir gauge between December 1, 2014 and March 31, 2015

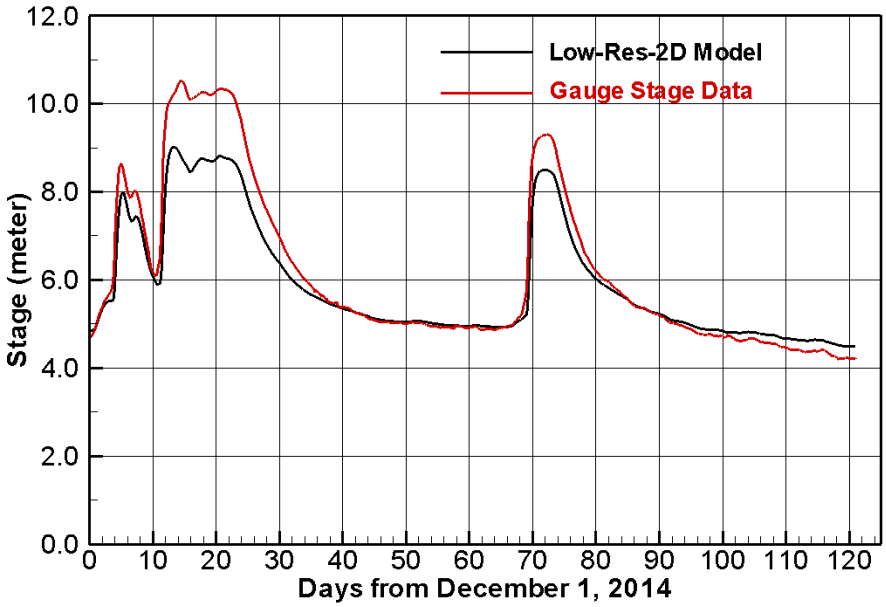

Figure 44. Comparison of simulated and recorded stage at Knight's Landing gauge between December 1, 2014 and March 31, 2015

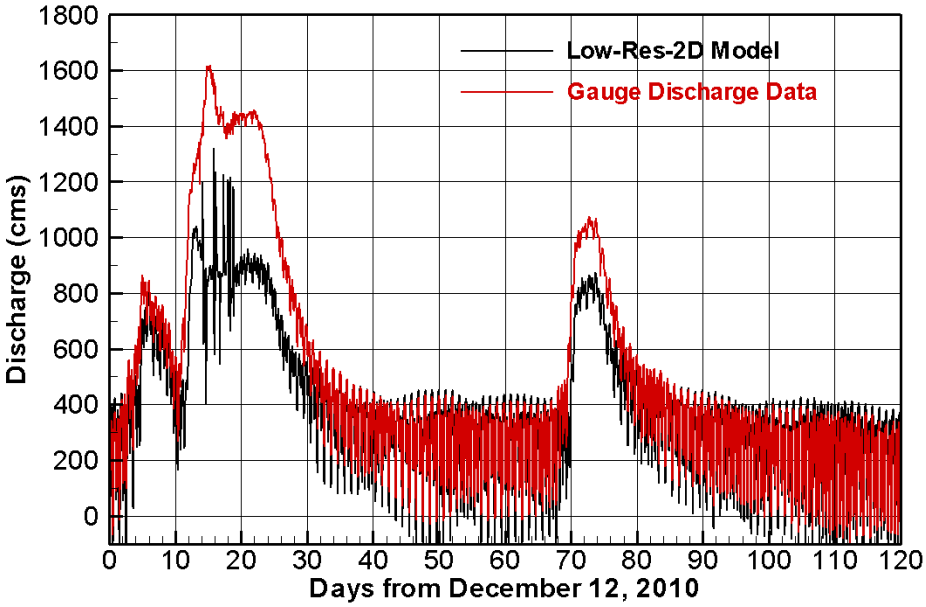

Figure 45. Comparison of simulated and recorded discharge at Freeport gauge between December 1, 2014 and March 31, 2015

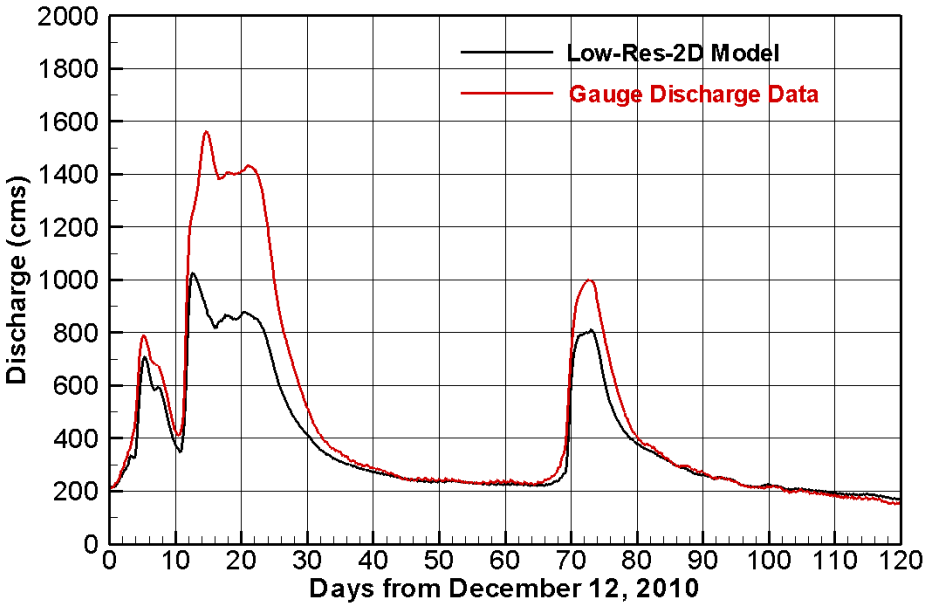

Figure 46. Comparison of simulated and recorded discharge at Verona gauge between December 1, 2014 and March 31, 2015

5.3 High Resolution Results

The horizontal extent of the High-Res-3D model mesh is actually a 2D mesh as discussed in Section 4.2. So SRH-2D simulation may be carried out for the period of December 1, 2014 – March 31, 2015 using the same conditions of the Low-Res-2D in Section 5.2. That is, the boundary conditions extracted from the Low-Res-2D model results may be used. This modeling run is named High-Res-2D1 model and may be used to compare with the Low-Res-2D results. The comparison offers an opportunity to evaluate the impact of mesh resolution on the model results. High-Res-2D1 run is to be carried out in FY 2016 and results will be compared in a future report. Later, another model run named High-Res-2D2 is used and described in 6.1.

6. High Resolution 3D Model Results

High-Res-3D model is developed to carry out 3D, non-hydrostatic, CFD simulation of the flow through a section of the Sacramento River from Knights Landing to Verona (see discussion in section 4.2). In FY 2015, the 3D modeling focuses on model validation which is achieved by comparing the model results with the ADCP data under the existing river conditions. After validation, the 3D model will be used to simulate scenarios with alternative Fremont Weir notch configurations. New river bathymetric survey, ADCP data collection and telemetry fish tracking have been carried out in 2015 and the new data are used for the model validation study.

6.1 2D Simulation Results

The horizontal extent of the High-Res-3D mesh is a 2D mesh as discussed in Section 4.2. A separate high resolution SRH-2D model run, named High-Res-2D1, is discussed in 5.3. Herein, another SRH-2D simulation is carried out for the period of December 1, 2014 – March 31, 2015. This run is named High-Res-2D2. The High-Res-2D2 run has the following purposes: (a) to select and verify appropriate boundary conditions for the High-Res-3D model; and (b) to provide the water surface elevation to the 3D model.

No calibration is performed with the High-Res-2D2 run. Instead, the same Manning's roughness coefficient as the calibrated Low-Res-2D model is adopted within the model domain. High-Res-2D2 adopts the modified boundary conditions described in Section 4.2.2 for the 2015 period. These same boundary conditions are used by the High-Res-3D model. The only difference between High-Res-2D2 and High-Res-2D1 is the different sets of boundary conditions used. The difference between High-Res-2D2 and High-Res-3D is that one is a 2D model and other is a 3D model.

The High-Res-2D2 predicted discharge is compared with the at Verona gauge data in Figure 47. The excellent match between the two is no surprising as the upstream discharge is computed from the discharge at Verona gauge subtracting out the flow contributions from the Feather River and other small inputs to the model domain. The match confirms that the time lag between Knights Landing and Verona is small enough to be neglected.

Figure 48 shows a comparison of the High-Res-2D2 results with the recorded stage at the Fremont Weir gauge. It is seen that the predicted and measured stages agree with each other very well, particularly in the high flow period. This is to our satisfaction as high flows in the Fremont Weir area are of primary interest for this study. It is also encouraging that the agreement is achieved without further model calibration with the Manning's coefficient. The stage at low flow is underpredicted, which suggests that the discharge used by the model through the Fremont Weir section may be lower than the actual value. Overall, we can conclude that the High-Res-2D2 results match well with the gauge data for the period of December 1, 2014 – March 31, 2015.

In the next section, High-Res-2D2 results are compared with the ADCP data, as well as the 3D model results. It will be shown that the 2D model predicts the depth-averaged velocity very well in comparison with the ADCP observed data. The High-Res-2D2 model is both calibrated and verified.

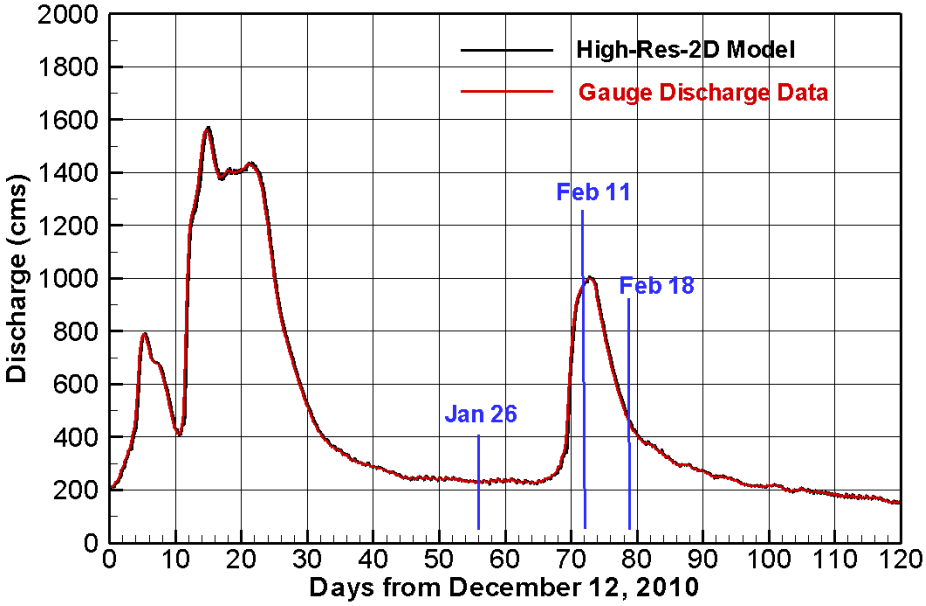

Figure 47. Comparison of High-Res-2D2 simulated and gauge discharges at Verona between December 1, 2014 and April 1, 2015

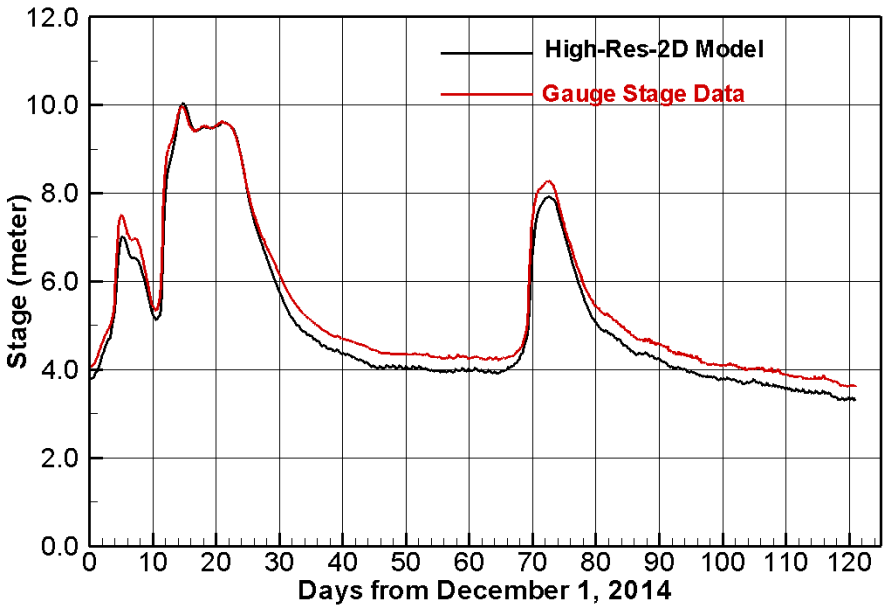

Figure 48. Comparison of High-Res-2D2 simulated and gauge stage at the Fremont Weir between December 1, 2014 and April 1, 2015

6.2 3D Model Results

ADCP data was collected by the DWR survey crew on three dates: January 26, February 11, and February 18, 2015 and the discharges at Verona station are marked in Figure 47. The daily discharge at Verona station is 232, 995, and 423 cubic meters per second, respectively, for the three days. Survey was carried out at ten river transects along the Fremont Weir section of the river as shown in Figure 49.

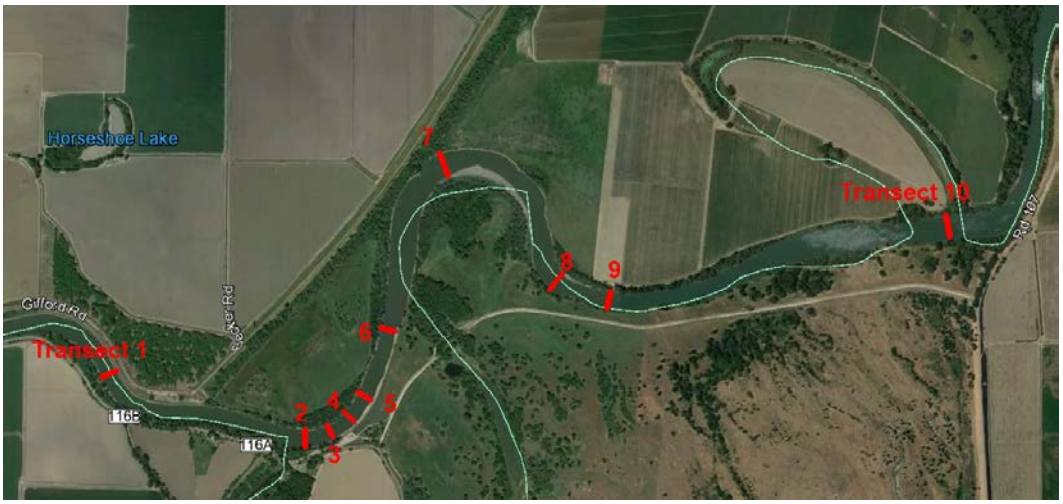

Figure 49. Ten (10) transects where the ADCP measurement was carried out in January-February, 2015

Two dates are selected for High-Res-3D modeling: January 26 and February 11, 2015 (see Figure 47). The January 26 represents a typical low flow condition (232 cubic meets per second), while February 11 is a relatively high flow condition (995 cubic meets per second). The two High-Res-3D runs are named Low-Q and High-Q runs, respectively. Validation using both low and high flows lends support to the accuracy of the 3D model over a range of flows.

6.2.1 Low Discharge Results

The Low-Q run corresponds to January 26, 2015 flow conditions. The 3D and 2D model results (High-Res-3D and High-Res-2D2) are compared with the ADCP data for the depth-averaged velocity at ten ADCP transects in Figure 50. Quantitative comparison will be made and reported in the FY 2016 report.

First, it is shown that 2D and 3D model results agree very well with the ADCP velocity data at most transects except for Transect 8. At Transect 8, the models predict that the maximum velocity remains near the left bank but the ADCP data shows that the maximum velocity has been shifted towards the center and the right bank. The probable cause for the mismatch is the high uncertainty of local river bathymetry used by the numerical models. This will be discussed next when the secondary flow patterns are compared later.

Second, it is found that 3D and 2D model results are very similar in most locations. This is a confirmation that 2D depth-averaged model is a very reliable tool in predicting the depth-averaged velocity for natural channels. If engineers are interested in the depth-averaged velocity only and if there are no major in-

stream geometrical features that may cause significant local flow changes, 2D model may be sufficient for flow prediction of a natural channel. A 3D model is needed only when there are in-stream structures in the model domain or one is interested in secondary flow patterns.

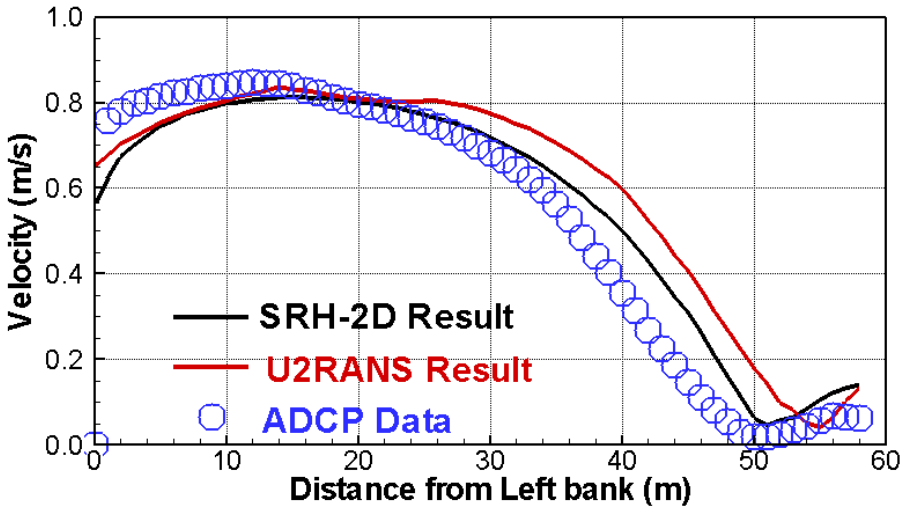

(a) Transect 1

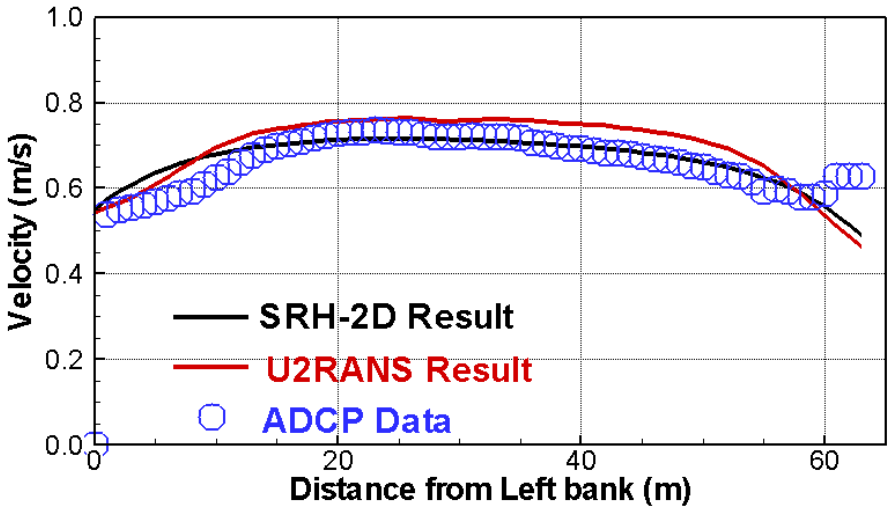

(b) Transect 2

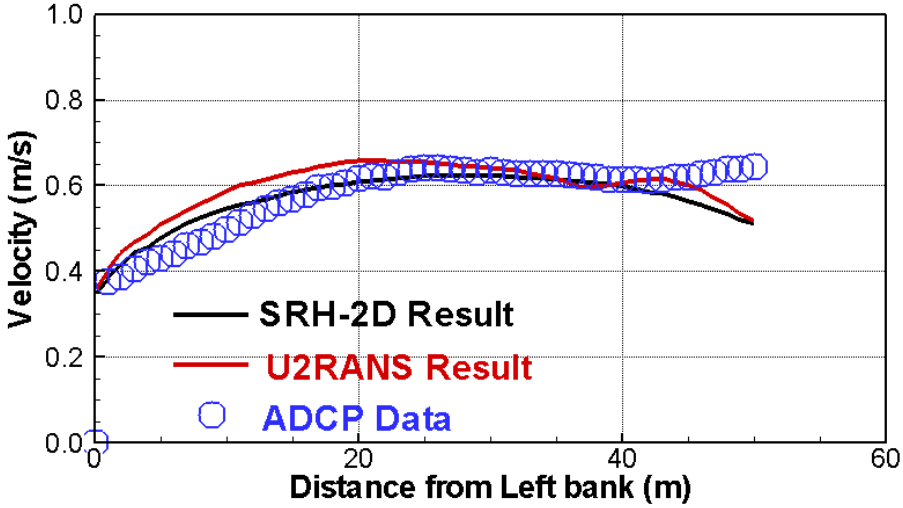

(c) Transect 3

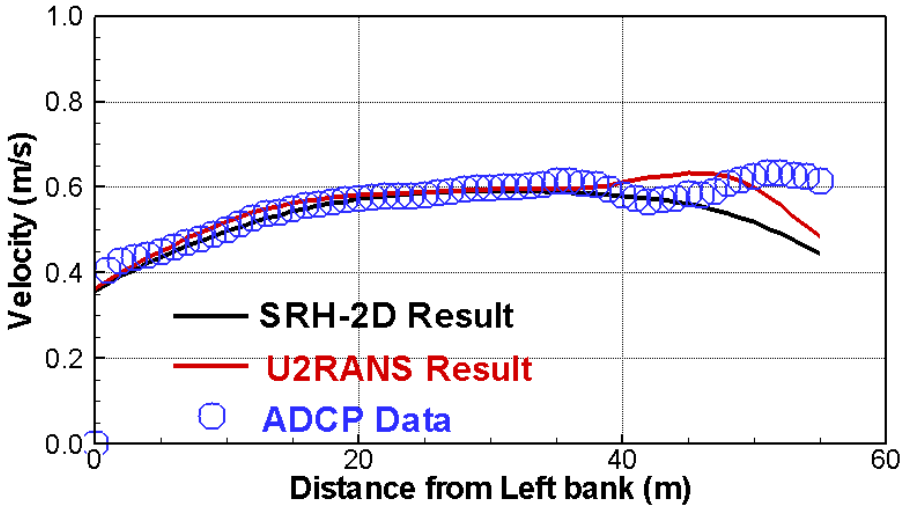

(d) Transect 4

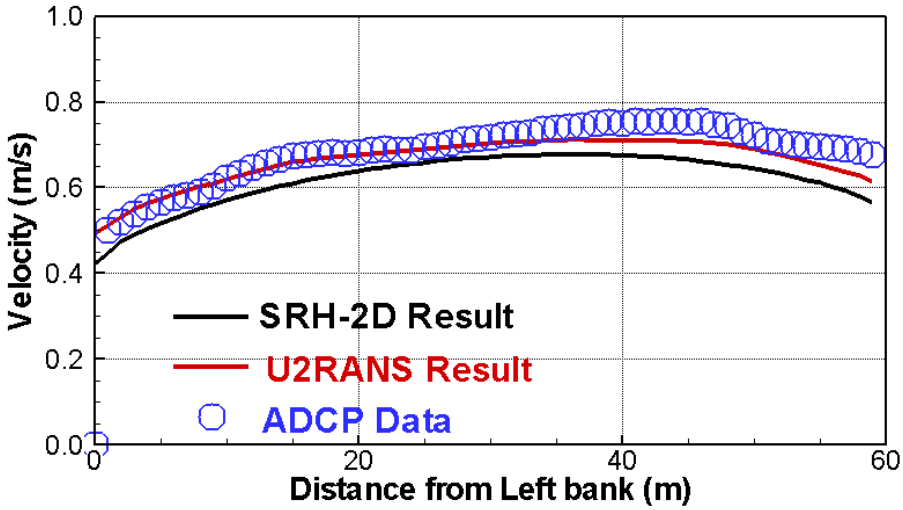

(e) Transect 5

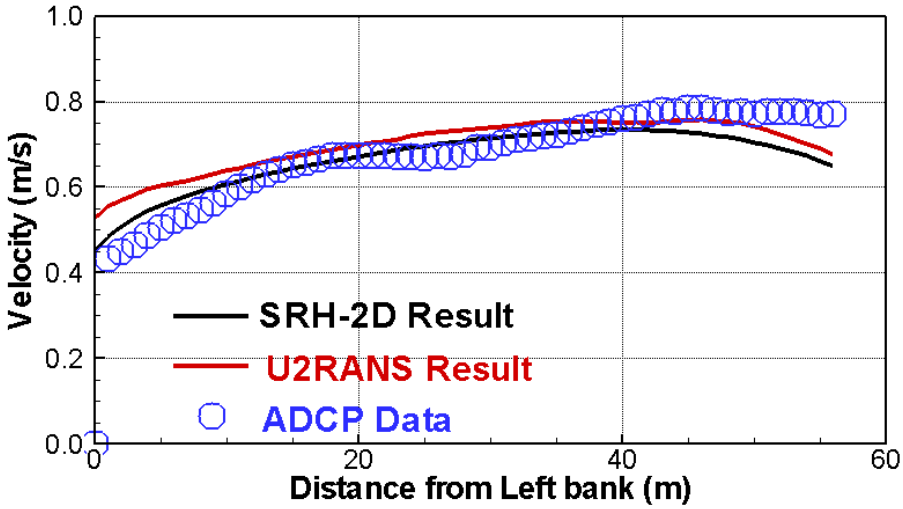

(f) Transect 6

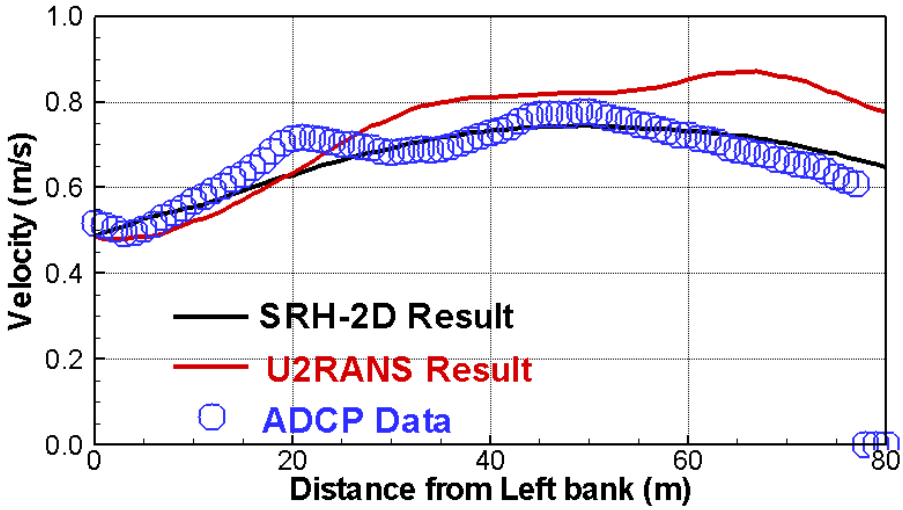

(g) Transect 7

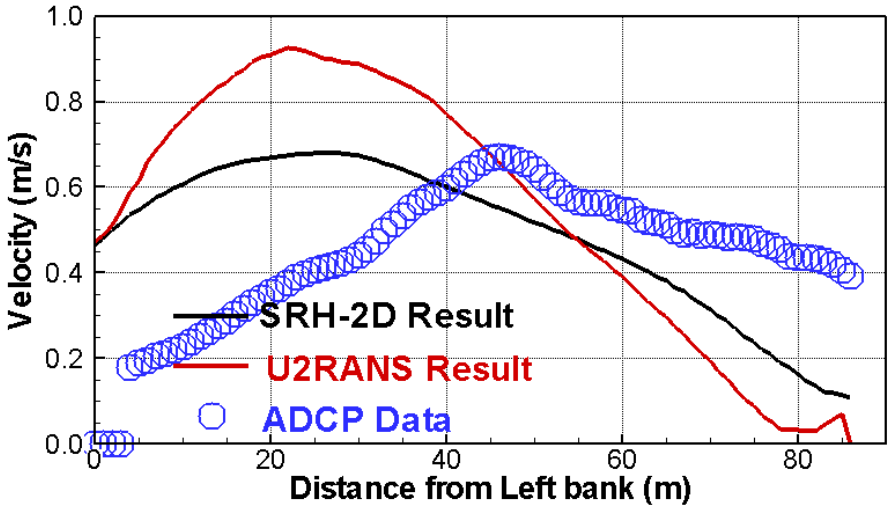

(h) Transect 8

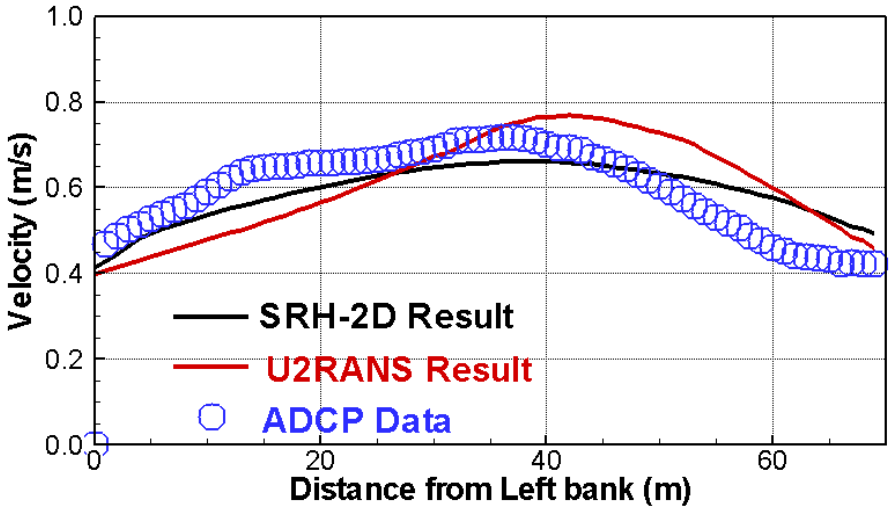

(i) Transect 9

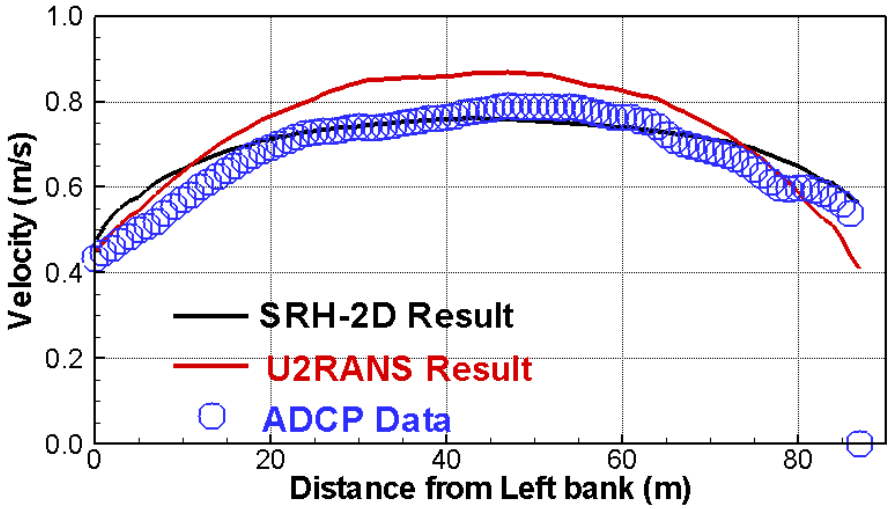

(j) Transect 10

Figure 50. Comparison of depth-averaged velocity along 10 transects between 3D, 2D and ADCP results for the Low-Q run on January 26, 2015

One of the advantages in using a 3D model is that secondary flow patterns may be predicted in a curved section of a channel even without in-stream structures. In the following, the 3D model predicted secondary flow patterns are compared with the ADCP data.

Secondary flows can be classified into two kinds: Prandtl's first kind (or pressure-driven) and Prandtl's second kind (or turbulence-driven). Pressure-driven secondary flows are induced by local pressure imbalances created by, e.g., flow curvature; while turbulence-driven secondary flows are due to anisotropy of turbulence normal stresses. Turbulence anisotropy may occur near sharp corners such as the corner of a square channel or across channels with transverse roughness changes. In general, pressure-driven secondary flows can reach 10% of the total flow velocity and is relatively easier to detect. A high resolution 3D model, such as U^2RANS, can predict the pressure-driven secondary flows reasonably. However, turbulence-driven secondary flows are typically small (about 1-2% of the main flow) and much harder to measure even in the laboratory environment. RANS models with two-equation turbulence models are also incapable of predicting turbulence-driven secondary flows. Therefore, the comparison of the present 3D model results with the ADCP data can only be done in a qualitatively sense and only overall patterns due to pressure-driven secondary flows may be examined. The ADCP measurement equipment in the field is not capable of measuring the turbulence-driven secondary flows accurately and the uncertainty in measuring the pressure-driven secondary flow is also high.

Predicted and ADCP measured secondary flow patterns are compared in Figure 51 at ten transects. The total velocity magnitude is also compared as color contours in the same figure. Some modeled transects show circulating secondary flows such as transects 1, 3 and 4; while recirculating secondary flows at other transects are not visible. It is not that there are no recirculating secondary flows on these transects; they are probably "overwhelmed" by the longitudinal (streamwise) flow. Secondary flows are much smaller in magnitude than the longitudinal velocity. Display of secondary flow patterns is not easy as transect has to be properly oriented so that it is as normal to the stream flow as possible. However, defining the "normal" of transect is hard for a natural river. Other ways of rearranging the transect orientation may display the secondary flow pattern better.

Overall, the 3D results agree with the ADCP data in qualitative secondary flow patterns at most transects except for transect 8. This is consistent with the comparison of the depth-averaged velocity. The mismatch in results at transect 8 (see Figure 51h) may be caused by the local river bathymetry. The cross section

bed elevation comparison shows that the river cross section used by the model is different from ADCP data. The ADCP cross section has a deeper thalweg and a higher right bar than the numerical model. Transect 8 is located near the exit of the big bend. It was reported by the survey crew that flow in this area was very unsteady and bed morphology may change significantly. This may explain why the bathymetry used by the model, surveyed at a different time, is different from the ADCP data bed profile.

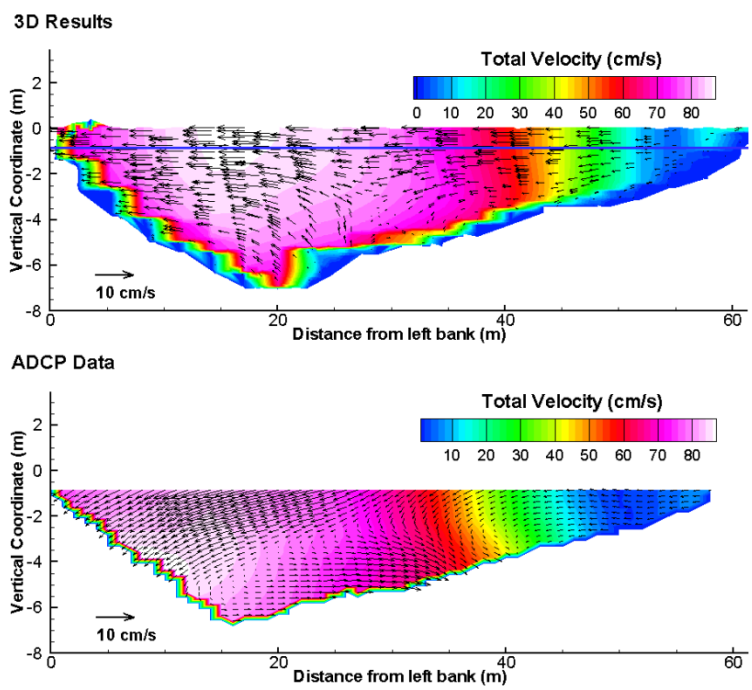

(a) Transect 1

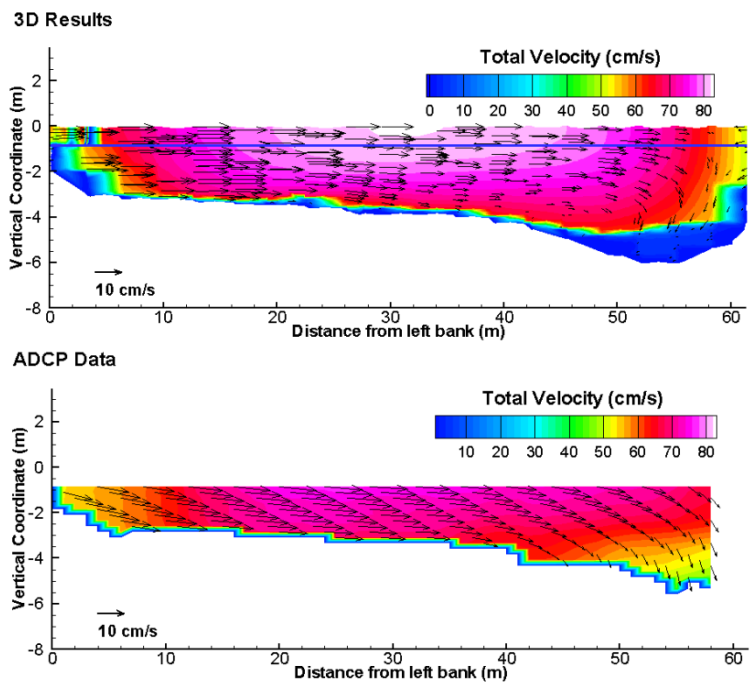

(b) Transect 2

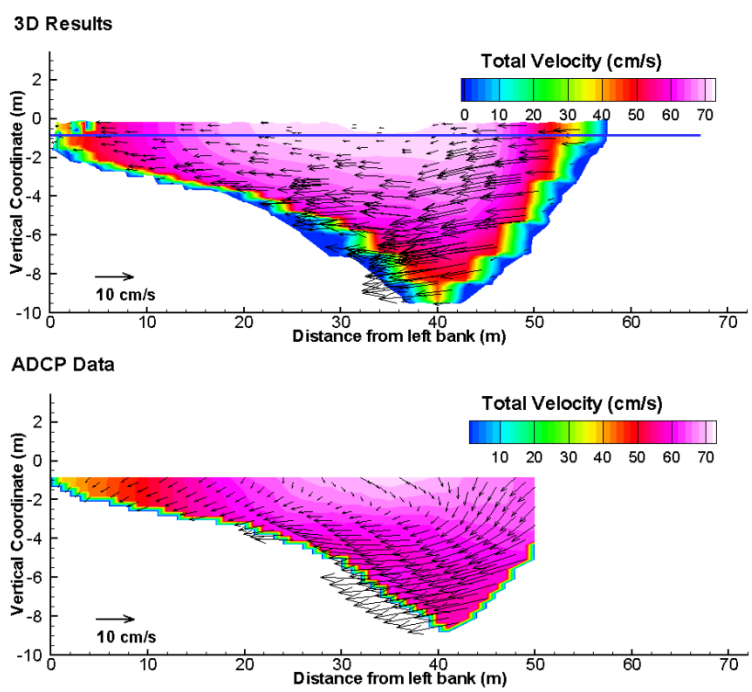

(c) Transect 3

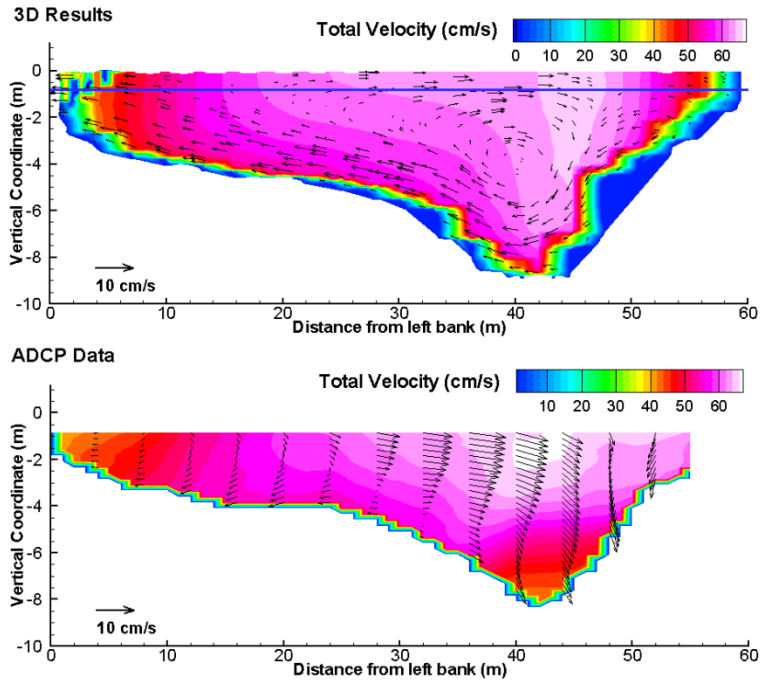

(d) Transect 4

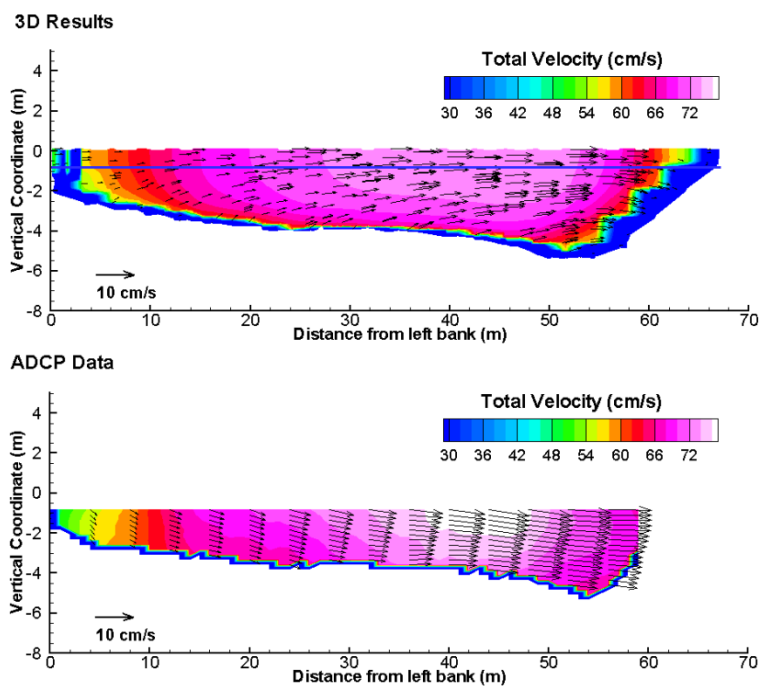

(e) Transect 5

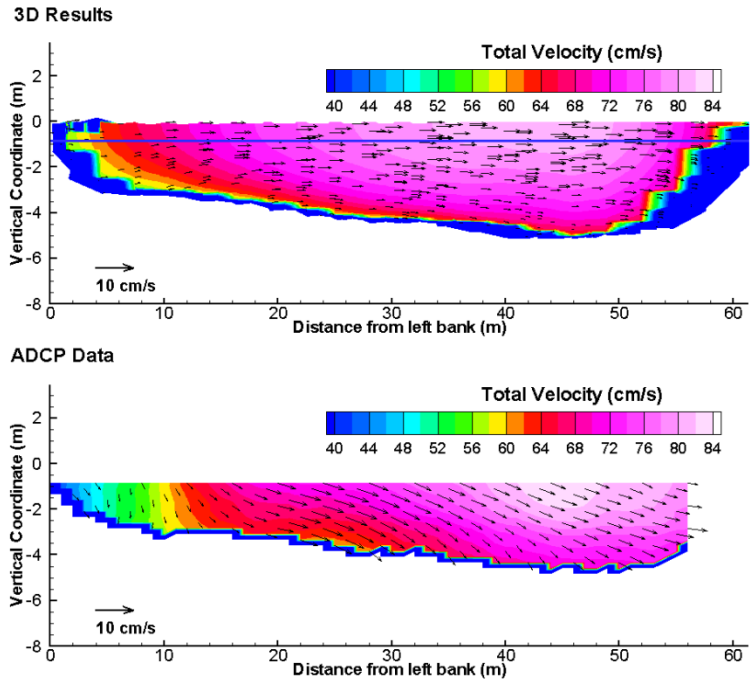

(f) Transect 6

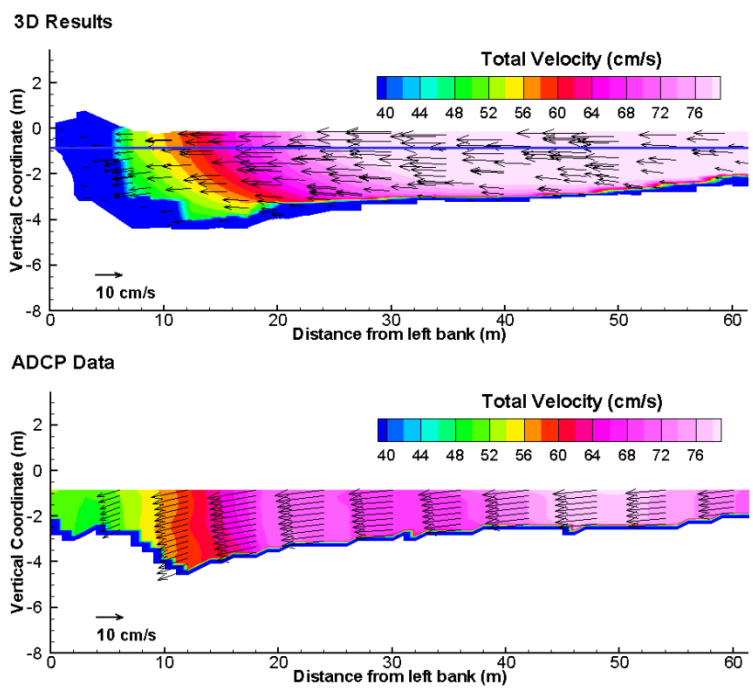

(g) Transect 7

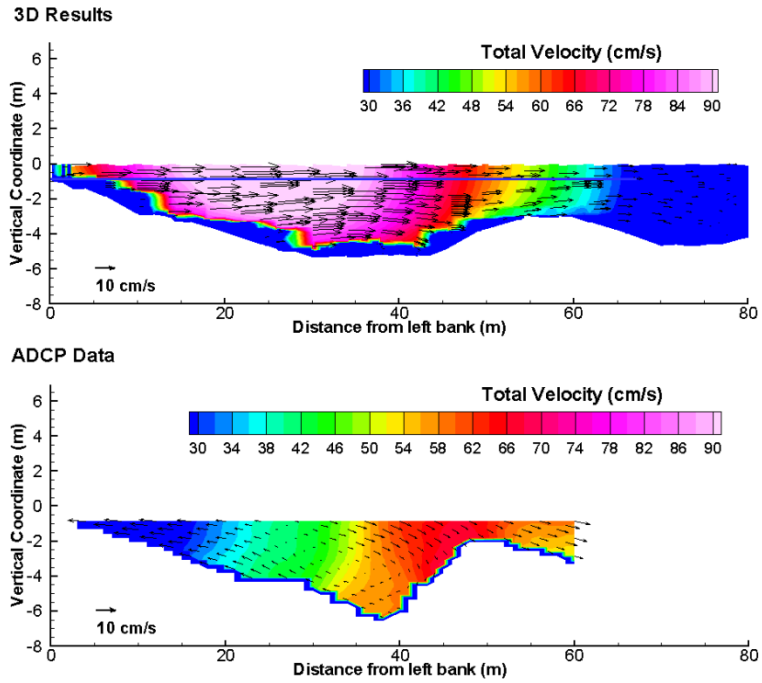

(h) Transect 8

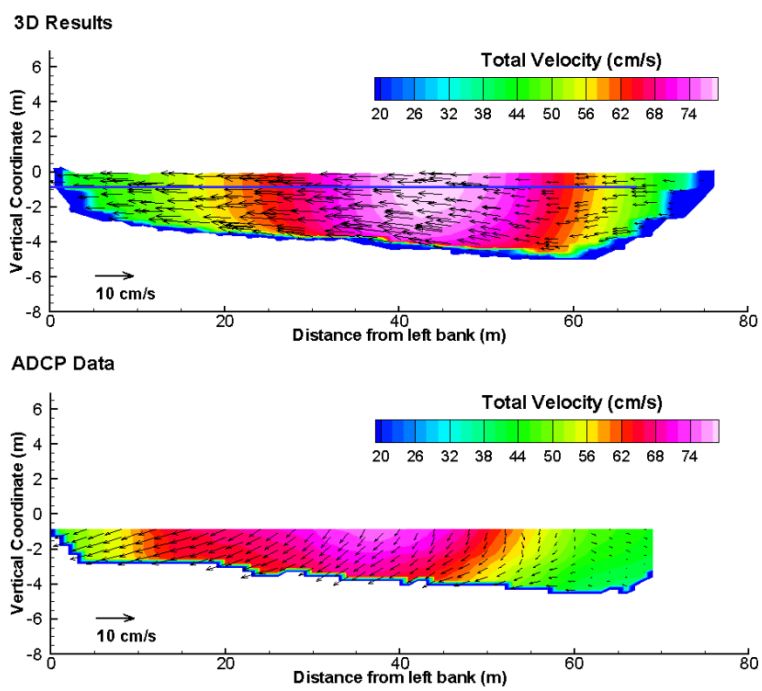

(i) Transect 9

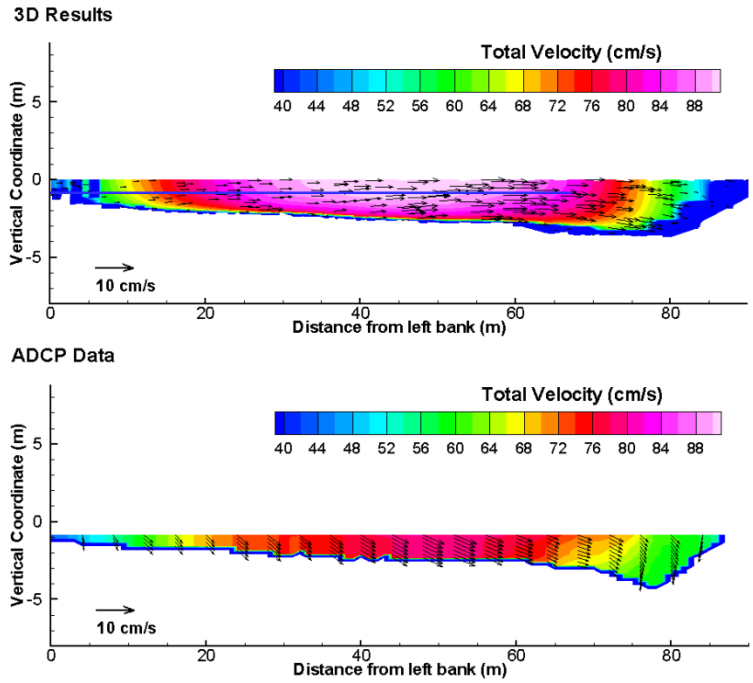

(j) Transect 10

Figure 51. High-Res-3D predicted (top) and ADCP measured (bottom) secondary flow patterns at 10 transects for the Low-Q run

6.2.2 High Discharge Results

The High-Q run corresponds to February 11, 2015 flow conditions. The 3D and 2D model results (High-Res-3D and High-Res-2D2) are compared with the ADCP data for the depth-averaged velocity at ten transects in Figure 50. Quantitative comparison will be made and reported in the FY 2016 report.

Overall, the conclusions reached with the Low-Q run still hold. That is, 3D and 2D model results agree well with the ADCP velocity data; and 3D and 2D model results also agree with each other well. Model comparison at transect 8 is much better than the Low-Q run. The local river bathymetry mismatch usually has a lesser impact on velocity than the Low-Q run.

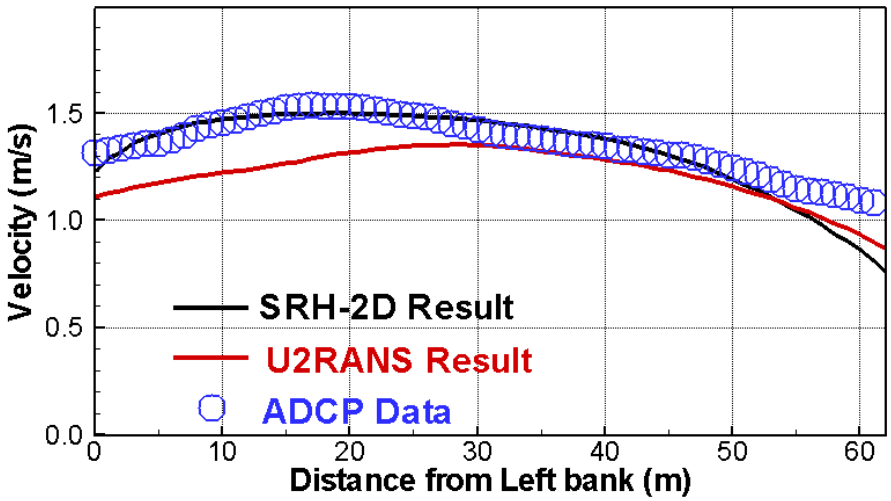

(a) Transect 1

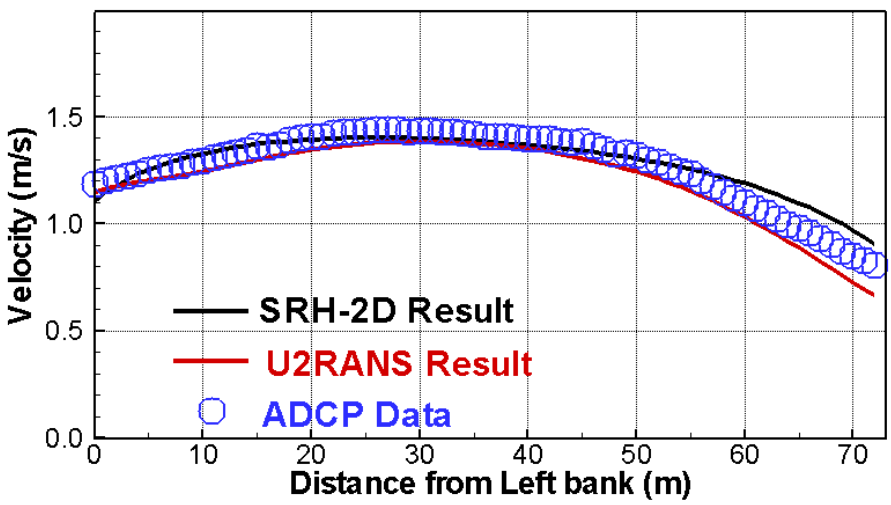

(b) Transect 2

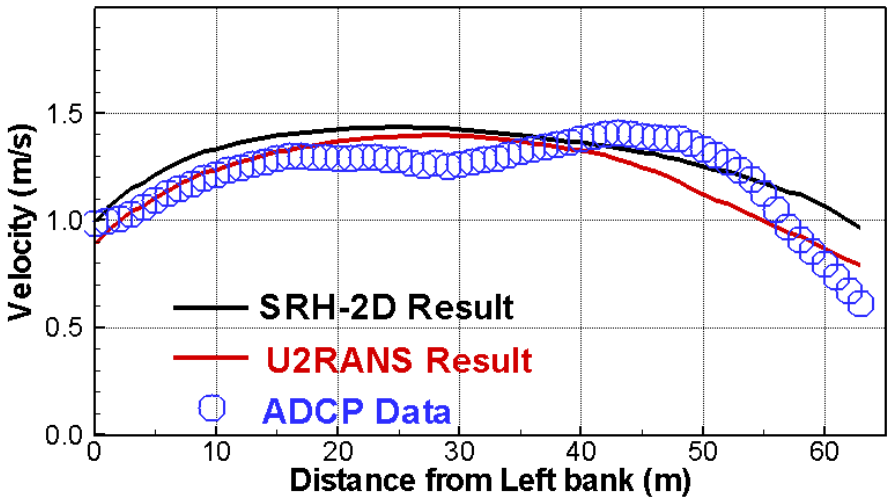

(c) Transect 3

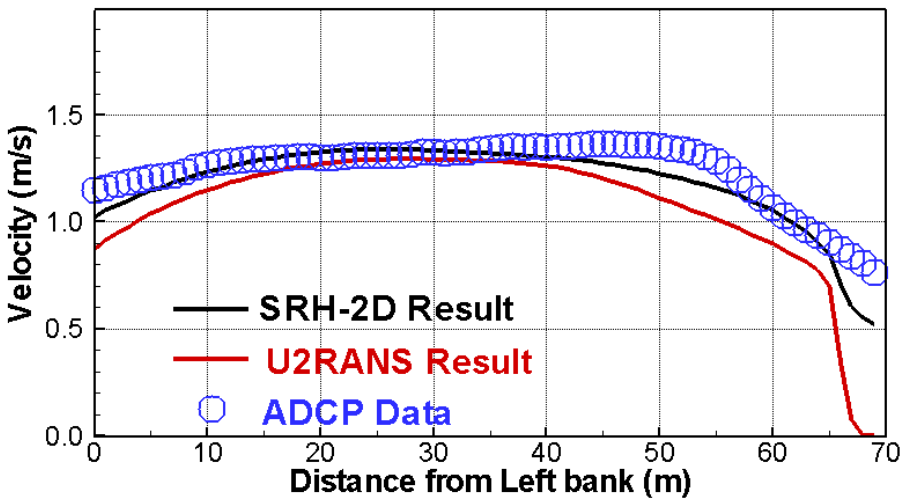

(d) Transect 4

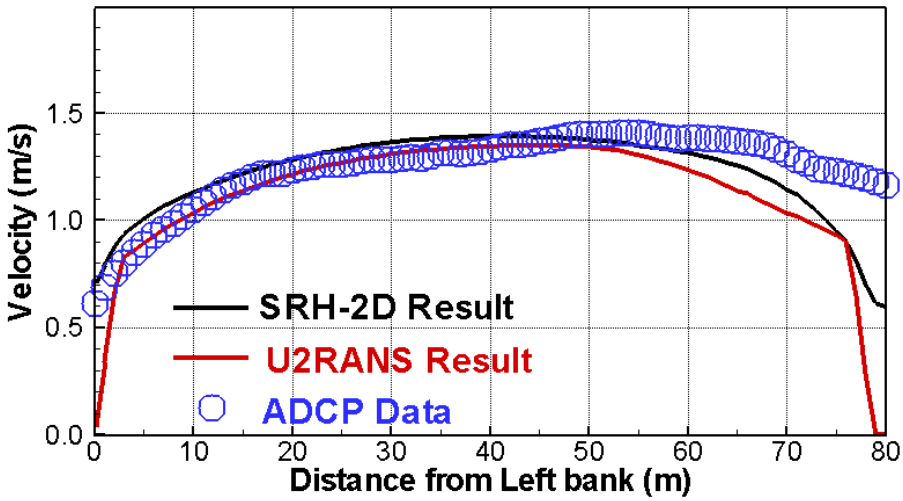

(e) Transect 5

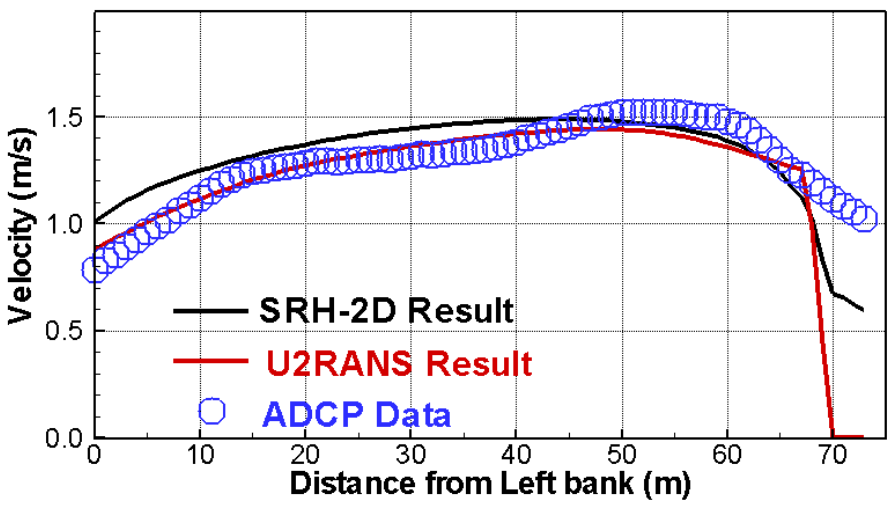

(f) Transect 6

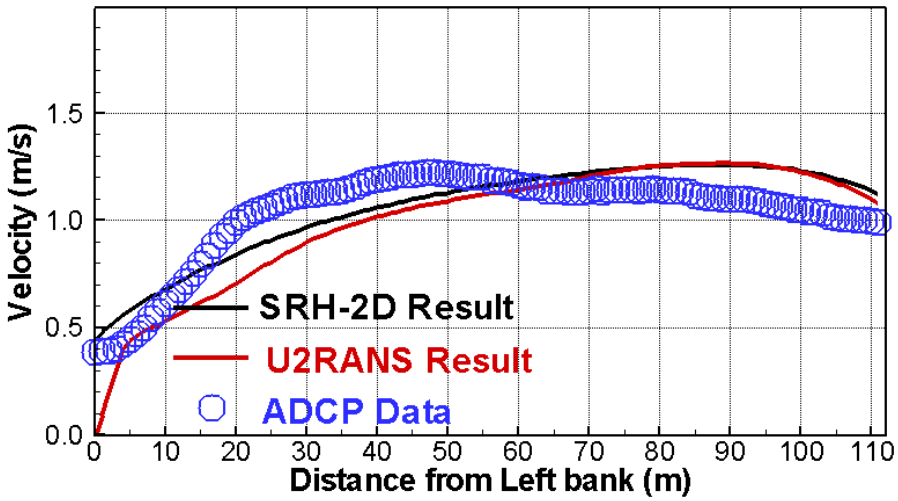

(g) Transect 7

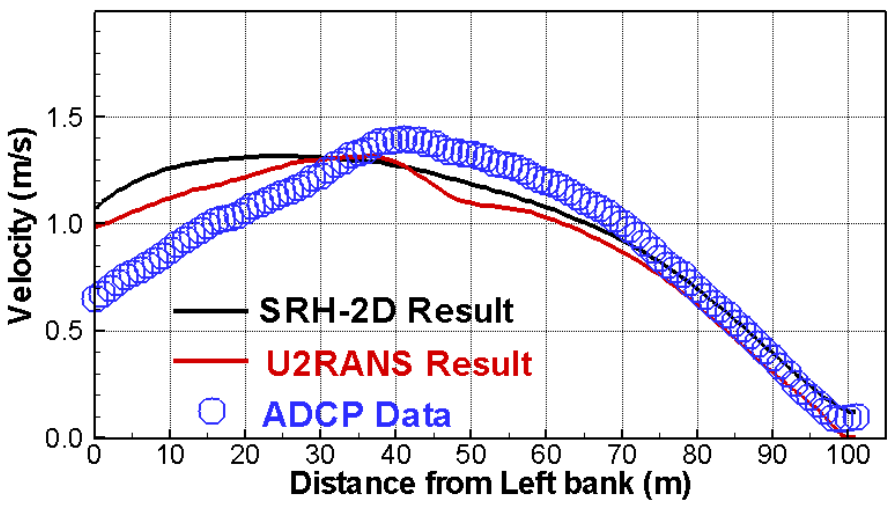

(h) Transect 8

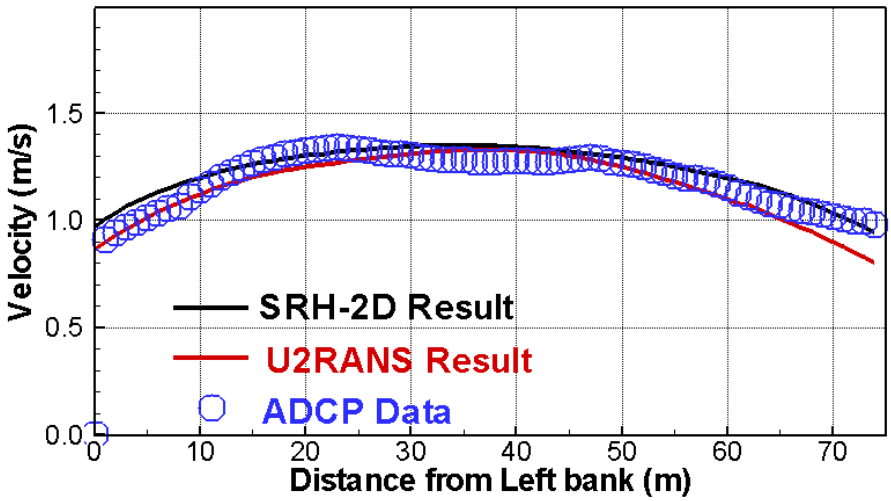

(i) Transect 9

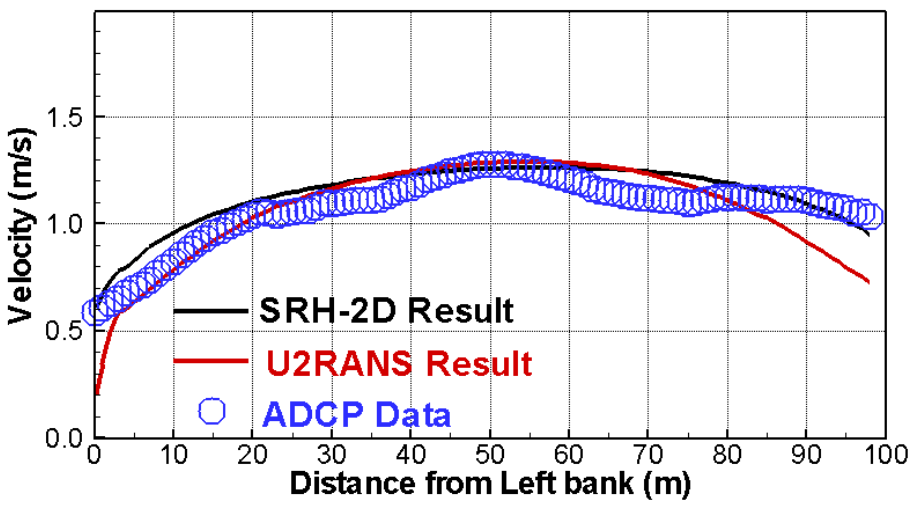

(j) Transect 10

Figure 52. Comparison of depth-averaged velocity along 10 transects between 3D, 2D and ADCP results for the High-Q run on February 11, 2015

Similarly, 3D model predicted secondary flows are compared with the ADCP data qualitatively in Figure 51 at ten transects. The total velocity magnitude is also compared in the same figure as color contours.

Overall, the 3D model predicted secondary flow patterns agree reasonably with the ADCP data at all transects.

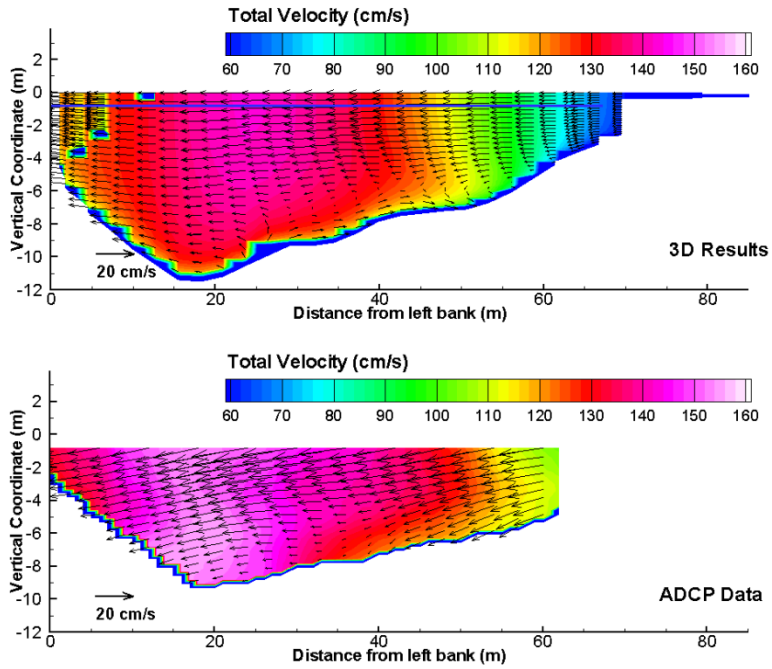

(a) Transect 1

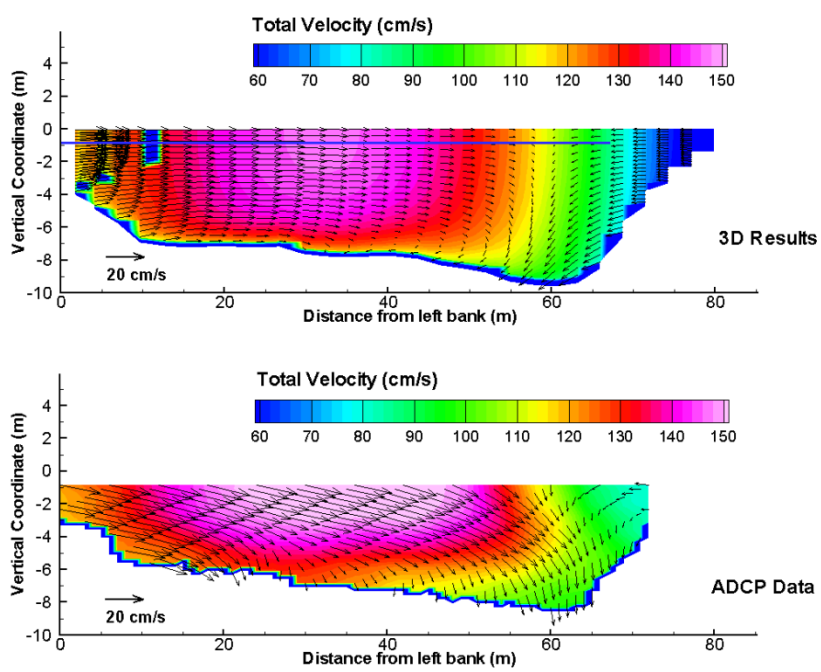

(b) Transect 2

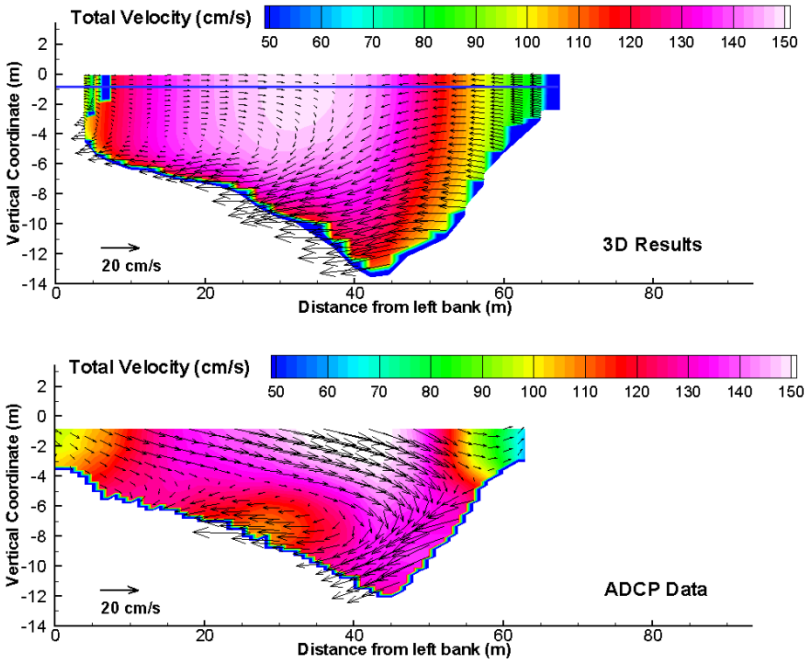

(c) Transect 3

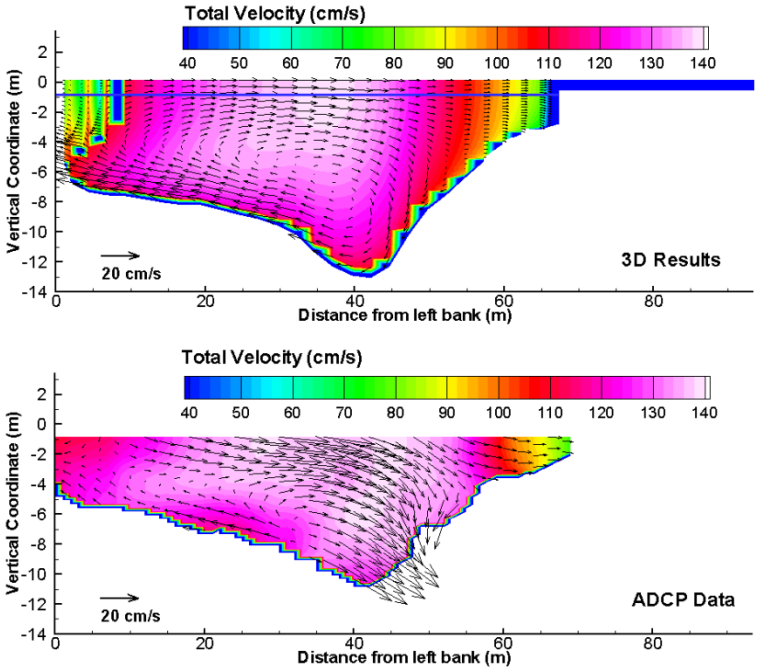

(d) Transect 4

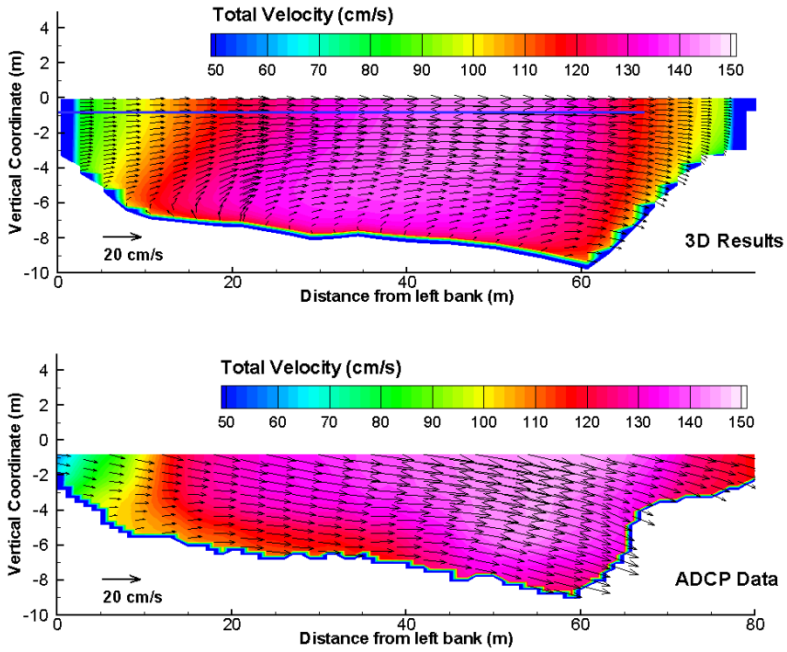

(e) Transect 5

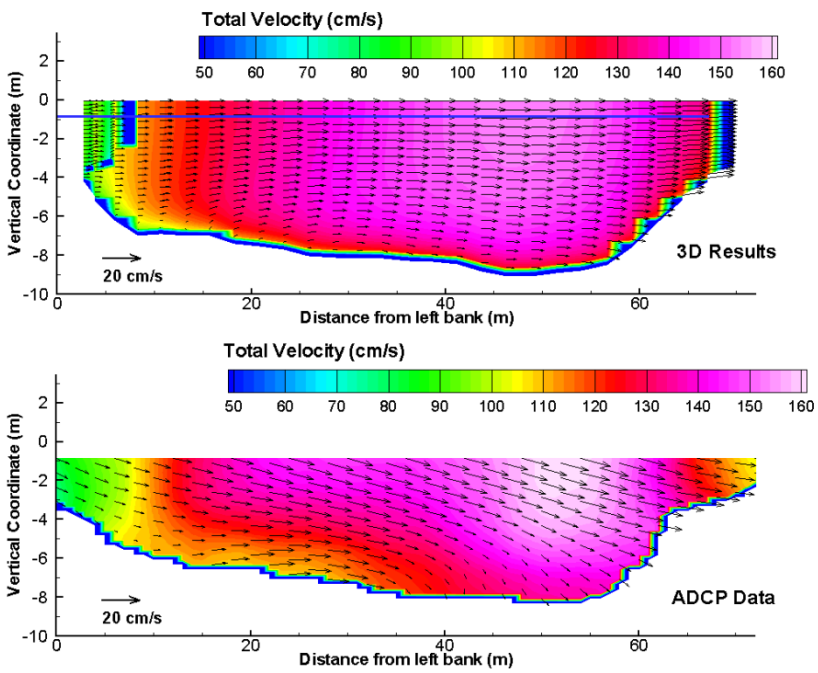

(f) Transect 6

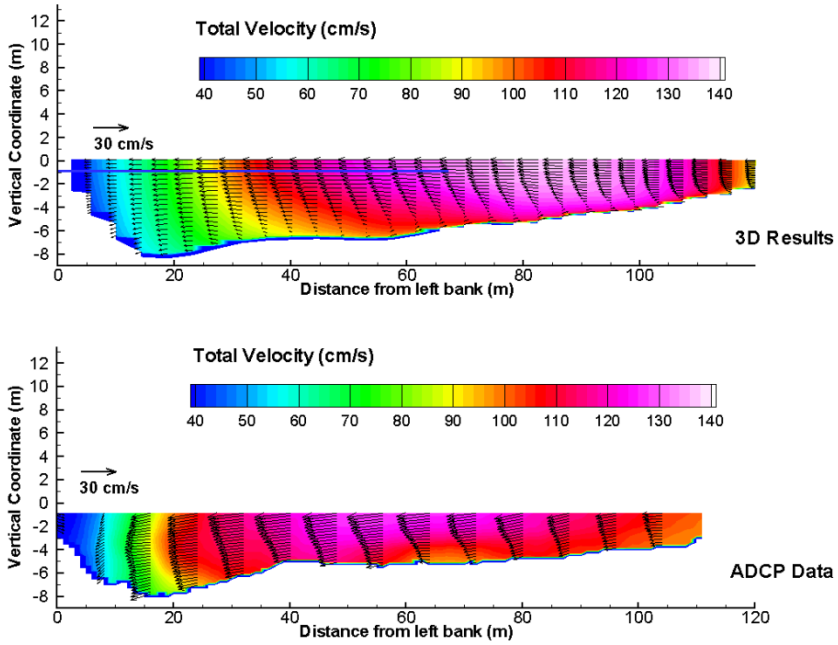

(g) Transect 7

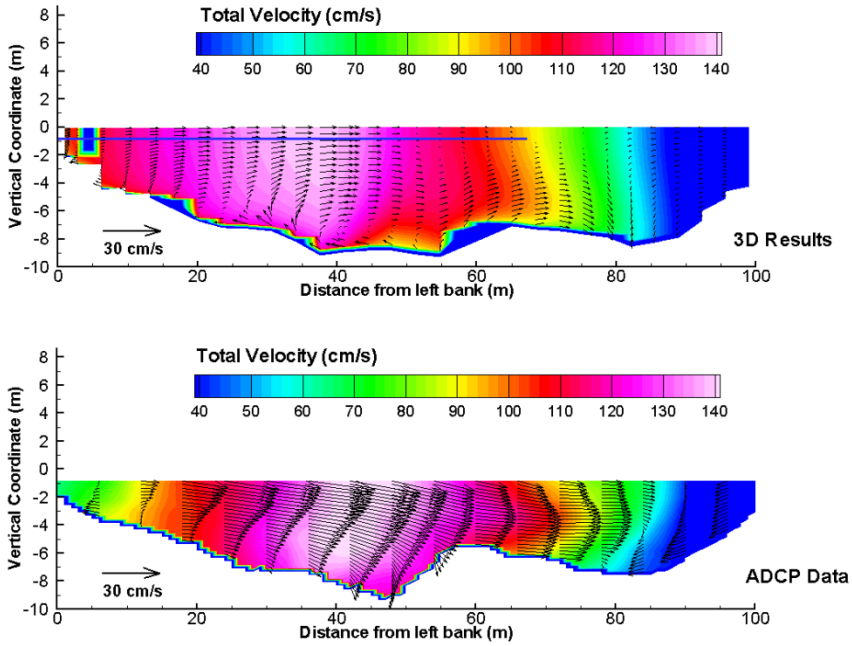

(h) Transect 8

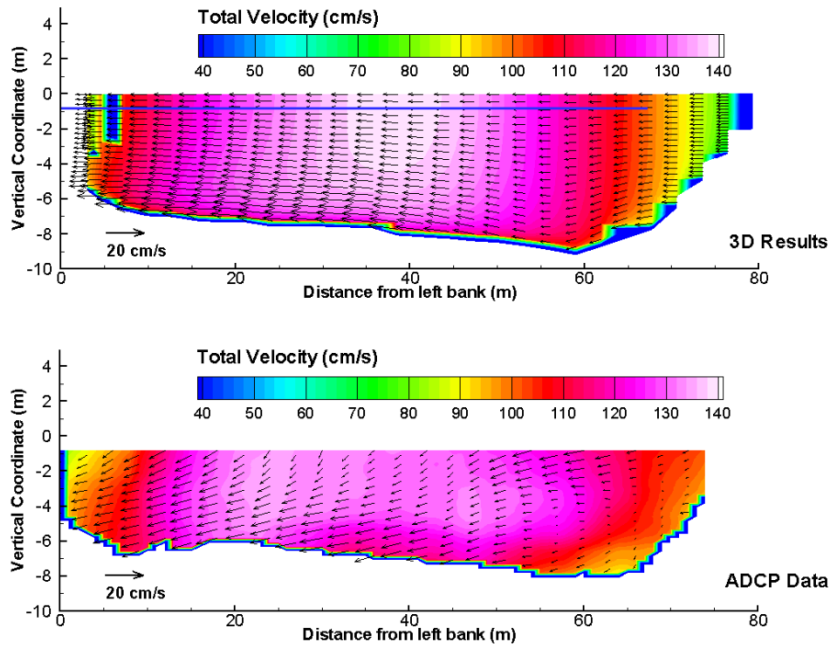

(i) Transect 9

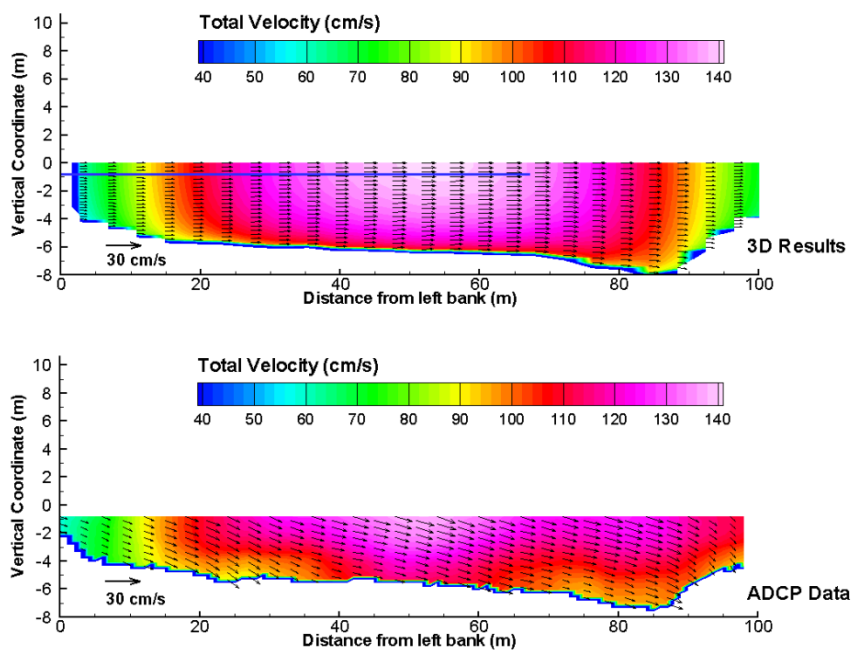

(j) Transect 10

Figure 53. High-Res-3D predicted (top) and ADCP measured (bottom) secondary flow patterns at 10 transects for the High-Q run

7. References

Dynamic Solutions LLC. (2011). Hydrodynamic Model of the Sacramento River from Freeport to Wilkins Slough using AdH and Delta EFDC-ELAM Model Linkage. Project Report, Knoxville, TN.

Greimann, B.P., Lai, Y.G., and Huang, J. (2008). "Two-Dimensional Total Sediment Load Model Equations," J. Hydraulic Engineering, ASCE, vol.134(8), 1142-1146.

Hall, B., Shvidchenko, A., Leclerc, R., Adams, L., Copeland, R., Cruey, B. (2010). Comprehensive Geomorphic and Sedimentation Analyses of Lower Sacramento River for Flood Management, Erosion Mitigation and Habitat Enhancement Design, 2nd Joint Federal Interagency Conference, Las Vegas, NV.

Hammack, E. A., Threadgill, T. L., Smith, D. L., & Sanborn, S. (2013a). Calibration of a Two-Dimensional Hydraulic Model of the Sacramento River Using a Coarse , Large Domain Mesh – Data Report. Vicksburg, MS.

Hammack, E. A., Threadgill, T. L., Smith, D. L., & Sanborn, S. (2013b). Calibration of a Two-Dimensional Hydraulic Model of the Sacramento River Using a Refined , Small Domain Mesh – Data Report. Vicksburg, MS.

Lai, Y.G. (2002). "User's Manual for U^2RANS: An Unsteady and Unstructured Reynolds Averaged Navier-Stokes Solver." IIHR draft document, University of Iowa.

Lai, Y.G., Weber, L.J., Patel, V.C. (2003a). "A non-hydrostatic three-dimensional method for hydraulic flow simulation - part I: formulation and verification," ASCE Journal Hydraulic Engineering, 129(3), 196-205.

Lai, Y.G., Weber, L.J., Patel, V.C. (2003b) "A non-hydrostatic three-dimensional method for hydraulic flow simulation - part II: application," ASCE Journal Hydraulic Engineering, 129(3), 206-214.

Lai, Y.G. (2008). SRH-2D Theory and User's Manual version 2.0, Technical Service Center, Bureau of Reclamation, Denver, CO.

Lai, Y.G. (2010). Two-Dimensional Depth-Averaged Flow Modeling with an Unstructured Hybrid Mesh. J. Hydraul. Eng., ASCE, 136(1): 12-23.

Lai, Y.G., and Greimann, B.P. (2010). Predicting contraction scour with a two-dimensional depth-averaged model. J. Hydraulic Research, IAHR, 48(3): 383-387.

Lai, Y.G., Greimann, B.P., and Wu, K. (2011). Soft bedrock erosion modeling with a two-dimensional depth-averaged model," J. Hydraul. Eng., ASCE, 137(8): 804-814.